AIP | Physics of Fluids

Wall-bounded turbulent flows at high Reynolds numbers: Recent advances and key issues

I. Marusic, B. J. McKeon, P. A. Monkewitz, H. M. Nagib, A. J. Smits et al.

Citation: Phys. Fluids **22**, 065103 (2010); doi: 10.1063/1.3453711

View online: http://dx.doi.org/10.1063/1.3453711

View Table of Contents: http://pof.aip.org/resource/1/PHFLE6/v22/i6

Published by the American Institute of Physics.

Wall-bounded turbulent flows at high Reynolds numbers: Recent advances and key issues

I. Marusic,[1] B. J. McKeon,[2] P. A. Monkewitz,[3] H. M. Nagib,[4,a)] A. J. Smits,[5] and K. R. Sreenivasan[6]
[1]*University of Melbourne, Victoria 3010, Australia*
[2]*California Institute of Technology, Pasadena, California 91125, USA*
[3]*Swiss Federal Institute of Technology Lausanne (EPFL), CH-1015 Lausanne, Switzerland*
[4]*Illinois Institute of Technology, Chicago, Illinois 60616, USA*
[5]*Princeton University, Princeton, New Jersey 08540, USA*
[6]*New York University, New York, New York 10012, USA*

(Received 17 February 2010; accepted 14 May 2010; published online 29 June 2010)

Wall-bounded turbulent flows at high Reynolds numbers have become an increasingly active area of research in recent years. Many challenges remain in theory, scaling, physical understanding, experimental techniques, and numerical simulations. In this paper we distill the salient advances of recent origin, particularly those that challenge textbook orthodoxy. Some of the outstanding questions, such as the extent of the logarithmic overlap layer, the universality or otherwise of the principal model parameters such as the von Kármán "constant," the parametrization of roughness effects, and the scaling of mean flow and Reynolds stresses, are highlighted. Research avenues that may provide answers to these questions, notably the improvement of measuring techniques and the construction of new facilities, are identified. We also highlight aspects where differences of opinion persist, with the expectation that this discussion might mark the beginning of their resolution.
 [doi:10.1063/1.3453711]

I. INTRODUCTION

We discuss aspects of our knowledge of incompressible, wall-bounded turbulent flows in an attempt to identify the key issues and challenges. The emphasis is on the behavior at high Reynolds numbers, and the discussion is directed to constant-pressure boundary layers as well as to pipe and channel flows. Recent advances, spurred by a series of international workshops and experimental studies, challenge current textbook orthodoxy and it therefore appeared useful to present them in this form. We have included alternative perspectives where appropriate. Our account focuses on the mean velocity distribution, fluctuations, as well as a hierarchy of turbulence structures. Beyond posing the questions believed to be important, we also identify avenues of research that may provide answers to these questions. We believe that these views will contribute to the improved understanding of wall-bounded turbulence based on first principles, and thus advance our ability to model, compute, and predict its behavior.

Given its practical importance, the topic of wall-bounded turbulent flows has received continuous attention since the formulation of the boundary layer concept. Almost from the start one important focus of research has been on the structure and scaling of wall turbulence at high Reynolds numbers. Clauser[1] and Coles and Hirst[2] presented comprehensive reviews of what is now commonly referred to as "classical" scaling. A relatively recent review of scaling issues is given by Gad-el-Hak and Bandyopadhyay.[3] In this view, which is largely related to the mean velocity behavior, the boundary layer is held to be composed of two principal regions that follow distinct scalings: a near-wall region where viscosity is important, and the outer region where it is not. On the basis of the mean momentum equation, the velocity and length scales in the near-wall region are taken to be $U_\tau=\sqrt{\tau_w/\rho}$ and ν/U_τ, respectively, where τ_w is the wall stress, ρ is the fluid density, and ν is the fluid kinematic viscosity. In the outer region, it is assumed that the appropriate length scale is the boundary layer thickness δ, or a scale related to δ, and the velocity scale continues to be U_τ, since U_τ sets up the inner boundary condition for the outer flow. In Townsend's approach,[4,5] for example, U_τ is regarded as a "slip" velocity seen by the outer scale motions and hence the appropriate scale for the *deviation* of the mean velocity from the free stream value of U_∞.

Hence, for zero-pressure-gradient (ZPG) turbulent boundary layers and flows in fully developed pipes and channels, the mean velocity profile is expressed[6] in the form of a law of the wall/law of the wake,

$$U^+ = f(y^+) + \Pi g(y/\delta). \tag{1}$$

Here, U is the mean velocity at a distance y from the wall and the superscript $^+$ indicates nondimensionalization using the friction velocity U_τ and the viscous length ν/U_τ. The parameter Π is referred to as the Coles wake factor. For pipe and channel flows, the same scaling is used by replacing δ by the radius of the pipe R or the half-channel height h. Close to the wall, the inner function $f(y^+)$ dominates: for $y^+\to 0$ the total shear stress is all viscous and $f(y^+)\sim y^+$ [with $g(0)=0$]. Further away from the wall the influence of viscosity diminishes, and if one assumes the existence of a region where

a)Electronic mail: nagib@iit.edu.

viscosity does not affect the mean-relative motions (and hence $\partial U^+/\partial y^+$), for smooth walls, the standard logarithmic profile is obtained from dimensional analysis and the Reynolds number invariance principle,[4,7]

$$U^+ = \frac{1}{\kappa}\ln(y^+) + B. \tag{2}$$

Alternatively, the classical log law is obtained from an overlap argument following Millikan,[8] and the von Kármán constant κ, is regarded as universal, with the additive constant depending on the geometry (pipe, channel, or boundary layer) and the wall roughness.

We will momentarily discuss alternatives to the log law, but the beauty of this classical result is its simplicity, particularly given the complexity of the multiscale nonlinear problem at hand. The underlying assumption is that the inner and outer regions connect only through the common velocity scale U_τ, and the mean velocity data confirm, at some level, the accuracy of this simple notion.

A second important focus of research on wall-bounded turbulence was inspired by the observation of coherent structures in turbulent boundary layers, starting with the horseshoe eddies identified by Theodorsen,[9] subsequently coupled with the discovery by Hama *et al.*[10] and Kline *et al.*[11] of the near-wall streaks and their role in the turbulence production cycle. Townsend[4,5] was among the first to couple scaling theories with the notion of coherent organized motions, which were significantly advanced by Head and Bandyopadhyay[12] and Perry and Chong.[13] Major reviews on the topic of coherent structures have been presented by Cantwell,[14] Sreenivasan[15] and Robinson,[16] and more recently by Panton[17] and Adrian.[18] The study of coherent structures revealed that the turbulent motions in the near-wall region interact with motions in the outer region, sometimes quite violently, as in sudden eruptions of near-wall fluid into the outer region (bursting) and the apparent modulation of near-wall motions by the passage of outer layer structures. The concept of "active" and "inactive" motions was advanced by Townsend[4,5] and Bradshaw[19] to distinguish the motions that contribute to wall-normal velocity fluctuations v and the momentum transport (thought to scale with the wall distance y perhaps coupled to the heads of the horseshoe eddies), from the motions that contribute primarily to the wall-parallel velocity fluctuations u and w ("sloshing" motions induced on a scale commensurate with y and δ).

Given this more recent background, it is not surprising that distributions of the turbulence intensity, particularly the streamwise component $\overline{u^2}$, do not scale according to the simple inner-outer arguments that seemed to work so well for the mean velocity profile. Further, $\overline{u^2}$ near the wall does not appear to collapse in inner layer variables and shows a significant dependence on Reynolds number (see Fig. 1). In addition, some authors have reported the appearance of a peak in the outer layer distribution of $\overline{u^2}$ at high Reynolds numbers, as shown in Fig. 2. In contrast, the spacing of the near-wall streaks seems invariant with Reynolds number, as seen in Fig. 3.

These observations raise obvious questions on how to

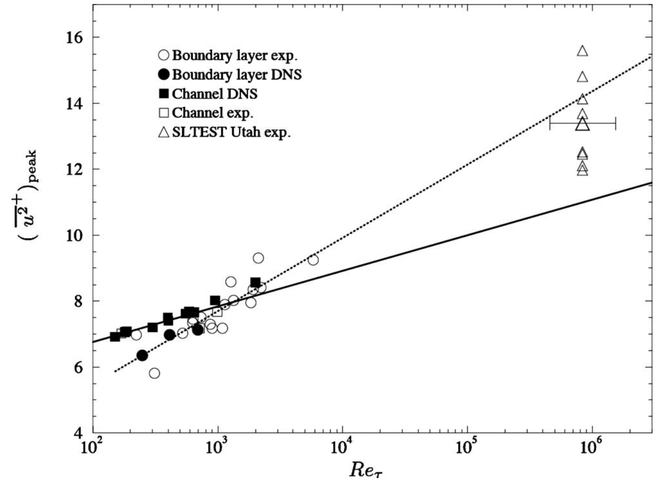

FIG. 1. Variation of the peak value of the inner-scaled streamwise turbulence intensity with Reynolds number (which occurs around $y^+ \approx 15$). The solid symbols are DNS results, and the open symbols are experimental. The circles indicate boundary layers, the squares are channels, and the triangles are for ASL data. The sources for the data are as given by Marusic and Kunkel (Ref. 20) and Metzger and Klewicki (Ref. 21). The lines indicate possible trends in the data, with the differences between the lines indicative of the estimated uncertainties.

scale and model turbulence in wall-bounded flows. Similarly interesting questions have been raised in recent years on the structure. For example, measurements of spectra have revealed the presence of previously unsuspected very large scale motions (VLSMs) that contribute significantly to the total energy content at all positions away from the wall. Although their origin and nature are yet to be fully revealed, they are associated with a peak in the premultiplied streamwise spectrum at low wave numbers (Kim and Adrian[26]) and have a characteristic scale that is of the order of 10δ ($\approx 10R$ in pipes), as shown in Fig. 4. The VLSMs can contribute as much as half the energy at high Reynolds numbers (Marusic[28] and Balakumar and Adrian[29]).

Why did such major features of wall-bounded turbulence become apparent only so recently? Part of the reason is that the past decade or so has witnessed considerable research at high Reynolds number. This emphasis on high Reynolds number has triggered the construction of major new experimental facilities and advances in experimental diagnostics, as well as direct numerical simulations (DNS). Recent high-Reynolds-number wall-bounded flow facilities notably include the Princeton *Superpipe* (Zagarola and Smits)[30] and the development of *SLTEST*, a site on the salt-flats of the Great Salt Lake Desert in Utah (Klewicki *et al.*[31]). High-Reynolds-number boundary layer facilities were also initiated in Chicago (Nagib *et al.*[32]), Stockholm (Österlund *et al.*[33]), Lille (Carlier and Stanislas[34]), Melbourne (Nickels *et al.*[35]), and Stanford (DeGraaff and Eaton[36]). At the same time, new experimental techniques, such as multiplane particle image velocimetry (PIV) and variants thereof have become mainstream diagnostic tools and have been successfully used to study wall turbulence (Adrian *et al.*,[37] Tomkins and Adrian,[38] Kahler,[39] Ganapathisubramani *et al.*,[40] Hambleton *et al.*,[41] Carlier and Stanislas,[34] Elsinga,[42] etc.). On the computational side, the DNS of channel flow (Moser

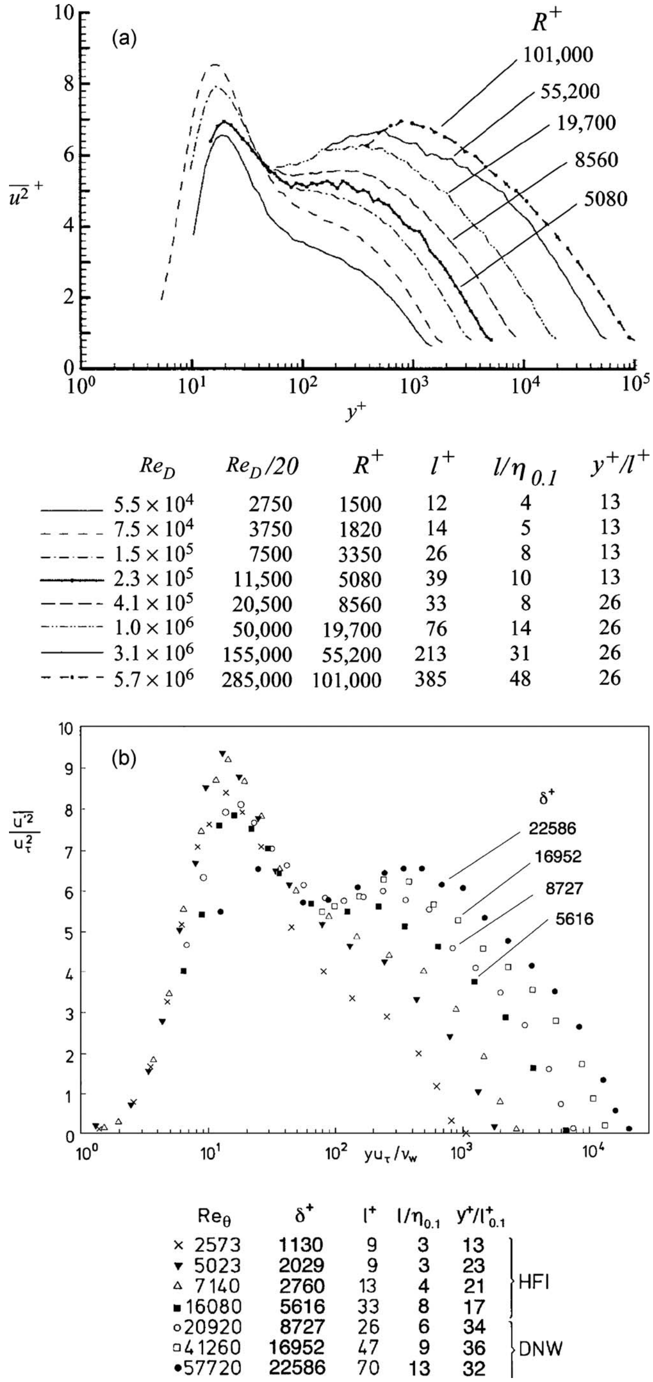

	Re_D	$Re_D/20$	R^+	l^+	$l/\eta_{0.1}$	y^+/l^+
———	5.5×10^4	2750	1500	12	4	13
- - - -	7.5×10^4	3750	1820	14	5	13
-·-·-	1.5×10^5	7500	3350	26	8	13
━━━	2.3×10^5	11,500	5080	39	10	13
– – –	4.1×10^5	20,500	8560	33	8	26
-··-··-	1.0×10^6	50,000	19,700	76	14	26
———	3.1×10^6	155,000	55,200	213	31	26
- -·- -	5.7×10^6	285,000	101,000	385	48	26

Re_θ	δ^+	l^+	$l/\eta_{0.1}$	$y^+/l^+_{0.1}$	
× 2573	1130	9	3	13	HFI
▾ 5023	2029	9	3	23	HFI
△ 7140	2760	13	4	21	HFI
■ 16080	5616	33	8	17	HFI
○ 20920	8727	26	6	34	DNW
□ 41260	16952	47	9	36	DNW
● 57720	22586	70	13	32	DNW

FIG. 2. The top plot, taken from Morrison *et al.* (Ref. 22), shows $\overline{u^2}^+$ profiles in pipe flow. The bottom plot, taken from Fernholz and Finley (Ref. 23), shows the same for boundary layer data. The tables are from the respective references and indicate the Reynolds number range and measurement conditions.

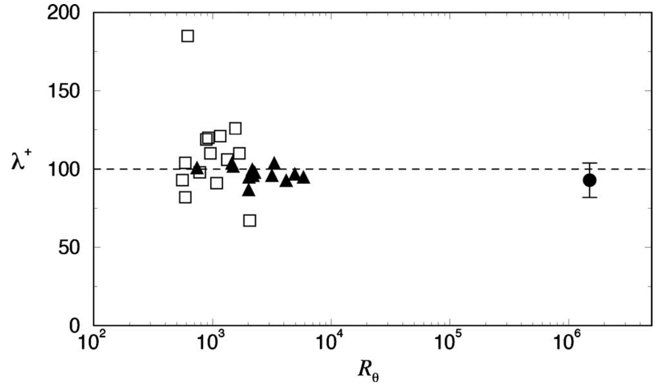

FIG. 3. Spanwise spacing of streaks in viscous sublayer, normalized by wall variables. Square symbols: data from Kline *et al.* (Ref. 11); filled triangles: Smith and Metzler (Ref. 24); filled circle: Klewicki *et al.* (Ref. 25).

et al.,[43] Abe *et al.*,[44] Iwamoto *et al.*,[45] del Alamo *et al.*,[46] Hoyas and Jimenez,[47] Hu *et al.*,[48] etc.) has offered new insights into the spatial organization and interactions of structures in the flow.

These developments have also led to a reanalysis and reassessment of the boundary-layer scaling at high Reynolds number and its asymptotic behavior. In addition to refinements of the classical scaling (see, e.g., Monkewitz *et al.*[49]), alternative theories have been proposed questioning the form and basis of classical scaling laws (Barenblatt *et al.*,[50] George and Castillo,[51] Klewicki *et al.*[52]). The ensuing debate on logarithmic versus power-law scaling of the mean velocity received considerable attention. With new experimental data at higher Reynolds numbers have come renewed questions related to the universality of the near-wall region and the influence of outer-flow motions. A recent, and comprehensive, survey of the state of research on the topic of scaling and structure in wall turbulence is given in a series of papers summarized by McKeon and Sreenivasan.[53]

In an attempt to resolve some of these new questions, and to reconcile subtle but important differences between various studies at the same nominal Reynolds numbers, a workshop was organized at Princeton University in October of 2003. Since then four followup workshops have been conducted in Trieste (2004), Chicago (2005), Erice (2006), and Baltimore (2008). Here, we present our perspective on the

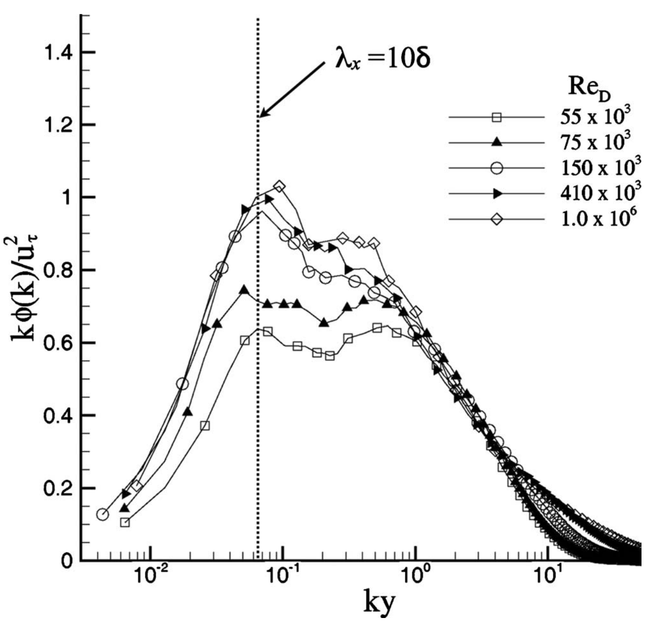

FIG. 4. Premultiplied streamwise velocity spectra at $y/R=0.1$ taken in the Superpipe for a range of Reynolds numbers. Figure is adapted from McKeon and Morrison (Ref. 27). The vertical line indicates the streamwise wavelength $\lambda_x/R=10$, corresponding to VLSMs.

TABLE I. Compilation of experiments considered extensively in the Workshops. OFI indicates oil-film interferometry, HW hot wires, ΔP pressure drop, κ is the von Kármán constant, and U_τ is the friction velocity.

Reference	Flow type	Highest Re_τ	κ	y^+: start of log law	No. of decades of log law	U_τ method	U meas. tech.
McKeon *et al.*[a] Morrison *et al.*[b] *Princeton Superpipe*	Pipe	300 000	0.421	600	1.8	ΔP	Pitot/HW
Monty[c] *Melbourne*	Pipe	4000	0.384	100	0.8	ΔP	Pitot/HW
Monty[c] *Melbourne*	Channel	4000	0.389	100	0.8	ΔP	Pitot/HW
Zanoun *et al.*[d] *Erlangen*	Channel	4800	0.37	150	0.8	ΔP	HW
Nagib *et al.*[e] *NDF, Chicago*	BL	22 000	0.384	200	1.4	OFI	HW
Österlund *et al.*[f] *KTH, Stockholm*	BL	14 000	0.38	200	1.0	OFI	HW
Nickels *et al.*[g] (2007) ICET (Duncan *et al.*[h]) *Melbourne*	BL	23 000	0.39	200	1.5	OFI	Pitot/HW
Metzger & Klewicki *SLTEST, Utah*	BL	$\mathcal{O}(10^6)$	⋯	⋯	~3	⋯	HW

[a]Reference 54.
[b]Reference 22.
[c]Reference 55.
[d]Reference 56.
[e]Reference 32.
[f]Reference 33.
[g]Reference 57.
[h]Reference 58.

new insights gained from these workshops. We aim to synthesize the main points and highlight the issues that need to be resolved, without presenting a comprehensive review of all the topics. We also consider other recent advances and point out where important differences of opinion persist, so as to mark the beginning of their resolution.

II. HIGH-REYNOLDS-NUMBER EXPERIMENTS

The Reynolds number dependence of turbulence quantities, whenever observed, is generally weak, scaling with something like the log of the Reynolds number. Therefore, it is essential to have access to high-Reynolds-number flows or, even more invaluably, facilities that can achieve a large range of Reynolds numbers. Table I summarizes the principal sources of data with $\mathrm{Re}_\tau \geq 4000$ that have been considered during the workshops, where Re_τ is the friction Reynolds number, also called the Kármán number, defined as the ratio of the boundary layer thickness δ or pipe radius or channel half-height to the friction length scale ν/U_τ. Many of these sites have only come online in the past decade and, in addition, large facilities are at various stages of planning now. These include the CICLoPE pipe described by Talamelli *et al.*[59] and the New Hampshire wind tunnel.[60]

In addition to the access to the necessary facilities, accurate measurements are required to identify the often subtle scaling trends in wall-bounded flows. This may seem like an elementary statement to make, but since the largest scale of the flow (δ, R, or h) is fixed by the size of the facility, the viscous scale becomes small at high Reynolds number, and a major challenge to the experimentalist is to maintain a sufficiently small measurement volume to avoid spatially averaging the smallest scales. Accurate measurements also require particular attention to the details of calibration and the response of the instrumentation. Both of these issues will be considered in more detail when discussing the available experimental data. We first consider some specific aspects of the experimental facilities themselves.

A. Atmospheric surface layer data

The near-neutral atmospheric surface layer (ASL) has been a historic source of very high Reynolds numbers, and the establishment of the Surface Layer Turbulence and Environmental Science Test (SLTEST) site on the salt playa of Utah's Western desert by Metzger and Klewicki[21] and Metzger[61] has been very influential. The strategic importance of the near-neutral ASL is clear: it represents some of the highest Reynolds number conditions that can be achieved terrestrially (and without the stringent constraints on probe resolution imposed by smaller-scale boundary layers). There is evidence that the ASL near-wall turbulence (Metzger and Klewicki,[21] Marusic and Hutchins,[62] etc.) and pressure field (Klewicki *et al.*[63]) scale in a manner similar to the canonical turbulent boundary layer. At the least, the ASL anchors Reynolds number trends in ways that would not be possible otherwise.

It should be noted, however, that the experimental challenges of obtaining high quality ASL data are severe, and considerable effort has been spent assessing the suitability of the ASL as a model for the canonical boundary layer. Of major importance is the issue of statistical convergence arising from the nonstationarity of the ASL, specifically due to a limited period of near neutrality, wind speed, and direction. Other questions are the importance of thermal effects associated with the passage through near neutrality, fetch conditions (that is, topological and surface roughness variations), the upstream and "free stream" boundary conditions, and so on.

B. Wall shear stress data

For boundary layer flows, a major limitation is that there is still no sufficiently accurate way to measure the wall shear stress (and hence U_τ) for all surface conditions. One ideally needs an accuracy of perhaps $\pm 0.5\%$ or better (see Nagib *et al.*[32]) to draw definitive conclusions. Clearly, a Clauser chart approach cannot be used to test the validity of the log law as it assumes it *a priori*. Oil-film interferometry is perhaps the best direct measurement method but its accuracy is still limited to no better than $\pm 1\%$ to 2% (e.g., Ruedi *et al.*,[64] Fernholz *et al.*,[65] and Monkewitz *et al.*[49]). It is also limited to gas flows and nonrough surface conditions. For pipes and channels, the situation is more straightforward as the wall-shear stress is known for fully developed flows from the pressure drop along the length of the pipe or channel. However, channel facilities must have aspect ratios much larger than 10 to minimize side wall effects on the wall shear stress and on the flow field, in general. The experiments listed in Table I use an independent measure of wall-shear stress. The table shows the reported value of the von Kármán constant κ, the length of the documented log region, and where the log law is reported to begin. These issues will be discussed later in Sec. III B. Note that for historical reasons we refer to κ as a constant while it may indeed be a variable coefficient as discussed later.

C. Evolution from initial conditions

An important issue with respect to the experimental facilities is the evolution from initial conditions: the development length in pipes and channels and the effects of upstream history on the development of boundary layers. The fact that in many experiments these effects are not, or only incompletely, documented is one of the principal causes of past and present disagreements between different experiments and their interpretations.

1. Pipe and channel flows

An issue raised in connection with the design of the CICLoPE pipe by Talamelli *et al.*[59] was the minimum development length for a pipe or channel flow to be regarded as *fully developed*. The definition of fully developed requires that all mean flow quantities (that is, velocity field and pressure gradient) and all turbulence quantities (i.e., $\overline{u^2}$, spectra, skewness, flatness, etc.) should become independent of streamwise location. A survey of the existing literature on pipe flows reveals considerable variation in what is considered a sufficient development length, where many workers have chosen to go longer as a precaution (which is perhaps a wise decision if the option is available). For example, while Nikuradse[66] used $40D$, where D is the pipe diameter, Perry *et al.*[67] used $398D$, and Zagarola and Smits[30] used $164D$ based on an assessment of the Reynolds number dependence of the transition length, the development of the turbulent wall boundary layers and a large-eddy development length.

In response to this practical query, Doherty *et al.*[68] conducted a series of detailed experiments in the Melbourne pipe, the same facility originally used by Perry *et al.*[67] Hot-wire velocity profile measurements were made at streamwise intervals of $2.5D$ starting from the pipe entrance to a length of $228D$ for bulk Reynolds numbers of 10^5 and 2.0×10^5. They concluded that the mean velocity invariance was achieved at approximately $50D$, while higher order statistics (up to flatness) required $80D$ of development length. It is possible that longer development lengths will be required at higher Reynolds numbers, but the Melbourne experiments provide important guidance for large projects such as CICLoPE where the large pipe diameter ($D\approx 0.9$ m) would entail substantial costs for any extra length of pipe.

Similar experiments were also carried out by Monty[55] and Lien *et al.*[69] in the Melbourne channel flow facility to investigate the required development length for turbulent channel flow. Here only mean velocity profiles were measured and it was concluded that 130 channel heights of development distance were required for invariance of the mean velocity field for bulk Reynolds numbers ranging from 4.0×10^4 to 1.85×10^5. We do not fully understand the difference from the pipes. The challenge of a longer development length in channel flows, exacerbated by the requirements on the aspect ratio and the larger flow rate required to reach the same Reynolds number as in a pipe, makes the construction of truly high-Reynolds-number channel facilities exceedingly difficult; see Zanoun *et al.*[70] This is unfortunate in view of the emphasis given to this flow field in DNS of wall-bounded turbulence. As an outcome of this work, the DNS of pipe flows is being encouraged, and a few data sets are now becoming available (for example, Wu and Moin[71]).

2. Boundary layers

For ZPG boundary layers, issues related to streamwise evolution are considerably more complex. Discussions at the workshops, and a survey of existing literature, revealed that some confusion and disagreement still exists concerning the use of the term *equilibrium*, or what constitutes a *well-*

behaved flow. A strict definition of equilibrium according to Townsend[4] and Rotta[7] requires all mean-relative motions and energy-containing components of turbulence (for example, Reynolds shear stress and the turbulence intensities) to have distributions that become invariant with streamwise development when scaled with local length and velocity scales (see, especially, Narasimha and Prabhu[72]). Rotta[7] demonstrated that the only wall-bounded flow for which this can occur on a hydrodynamically smooth surface is the sink flow, and this condition was experimentally validated by Jones *et al.*[73]

In boundary layers other than the sink flow, not even the mean velocity can be described from the wall to the free stream by a function of a single similarity variable. At least two similarity variables, $y^+ = yU_\tau/\nu$ and y/δ are required. Therefore, the above strict definition of equilibrium needs to be relaxed: In the boundary layer one might speak of equilibrium when the mean velocity deficit $U_\infty - U$ in the outer part exhibits self-similarity, since this region dominates at large Reynolds numbers.

The commonly held view is that the mean-velocity profile in all ZPG boundary layers would be self-similar according to the above definition when the Reynolds number is sufficiently high. This stems largely from the interpretation of data correlations with Reynolds number, such as the one by Coles[74] for the wake factor Π, which becomes nominally constant for $\mathrm{Re}_\theta \gtrsim 8000$, Re_θ being the Reynolds number based on momentum thickness. Significant scatter in the data has led to questions about the validity of the experiments used in the correlation. It has also motivated new theories by Castillo and Johansson[75] and others to introduce additional parameters to explain the deviation of some data sets from classical scaling. Another possible explanation for the scatter is the rather strong dependence of Π on the method by which it is extracted from the data and, more generally, on how sensitive Π and δ are to the particular fit used for the outer part of the mean velocity profile (see Monkewitz *et al.*,[76] for a detailed discussion).

It is also important to keep in mind that each experimental (and computed) boundary layer must develop from a unique set of upstream boundary conditions. Here we are referring to inflow conditions and tripping/transition devices, and not to poorly designed experiments affected by high free-stream turbulence, three dimensionality, or spurious pressure gradients. For example, a boundary layer developing on a short plate at high speed may have the same Re_θ as a boundary layer developing on a long plate at low speed, but not necessarily the same value of the shape factor $H = \delta^*/\theta$ and/or of Π, unless the development length of both layers has been sufficient; see the recent discussions by Chauhan and Nagib[77] and Castillo and Walker.[78] What is the sufficient development length for a ZPG boundary layer to become independent of initial conditions? In general, this question is still open, but the answer must depend on the specific initial conditions, on the quantity being considered, and on the desired degree of independence, which needs to be quantified. In other words, a flow is not fully characterized by its Reynolds number alone.

Recent progress on the easier problem of quantifying the deviation from the canonical equilibrium state has been encouraging, largely because many of the new experiments obtained the wall stress by independent means, and have carefully documented the evolution of the boundary layer with downstream distance. However, additional data from different facilities are required before many of the questions can be answered satisfactorily, and this has become a focus for ongoing collaborative efforts. Significant advances have been made by Nagib *et al.*,[32] Chauhan *et al.*,[79] and Monkewitz *et al.*,[49] who have proposed criteria to quantify when ZPG boundary layers are well behaved. Their criteria are based on the assumption that the canonical asymptotic state is attained when Π reaches a constant value and/or *the values of skin friction and shape factor are consistent with each other in the framework of classical theory*. They argue that, once the asymptotic state is reached, the influence of initial conditions should appear only in a virtual origin, which is a correction of the nominal streamwise position $\hat{x}$ along the plate. Figure 5 shows how a large collection of existing data compares, with and without the virtual origin correction. The uncorrected data illustrate the high degree of variability among different experiments, as discussed above. The globally successful correction is based on the asymptotic boundary layer growth $\delta^*/x \sim \kappa^2/\ln^2(\mathrm{Re}_x)$ derived by Monkewitz *et al.*[49] from the log law without arbitrary data fitting.

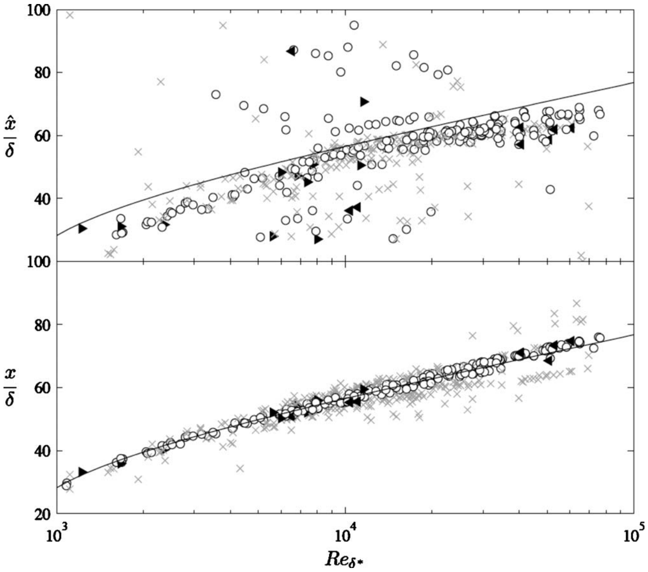

FIG. 5. Variation of normalized boundary layer development without $(\hat{x}/\delta)$, top part, and with correction (x/δ) for virtual origin (bottom). Taken from Chauhan *et al.* (Ref. 79). Here a total of 471 data points are shown, where the different symbols represents results that satisfy different levels of criteria according to Chauhan *et al.* (Ref. 79). "×" indicate where the criteria fail. The solid line is the theoretical result from Monkewitz *et al.* (Ref. 49) in conjunction with numerical integration of a composite profile fit to the mean velocity profile.

The more difficult problem of how the canonical asymptotic state evolves from an arbitrary initial condition was first tackled by Perry *et al.*[80,81] who computed the development of the ZPG boundary layer from a specified set of initial conditions using the momentum and continuity equations in simplified form. This involves the hypotheses that the total shear stress field is uniquely described by a two-

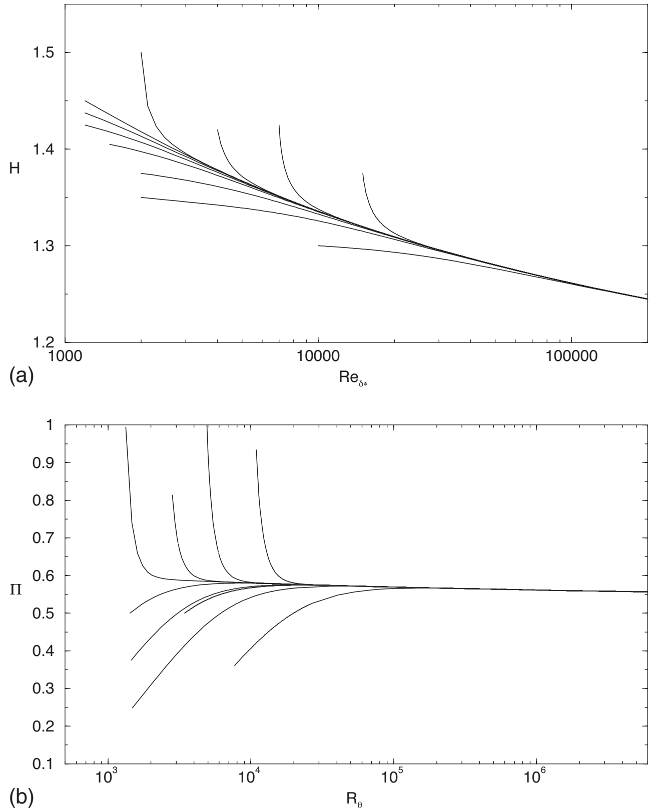

FIG. 6. Computed evolution of shape factor H and Coles wake factor Π vs Reynolds number for various initial conditions for ZPG boundary layers using the model of Perry *et al.* (Ref. 82).

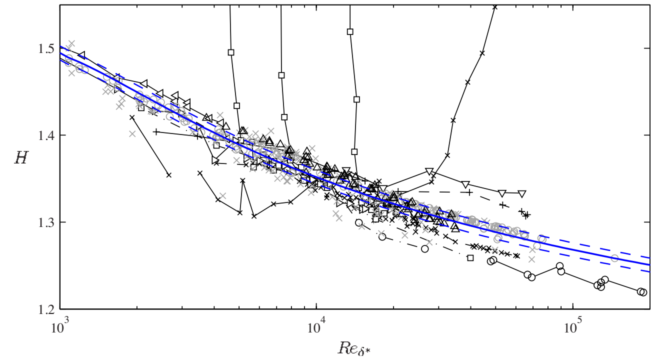

FIG. 7. (Color online) Variation of shape factor with Reynolds number in boundary layers evolving toward zero pressure gradient [from Chauhan *et al.* (Ref. 77)], and at nominally ZPG conditions [Chauhan *et al.* (Ref. 79)]. The solid line is obtained by numerical integration of a composite profile description of the mean velocity profile given in the latter reference, with dashed lines indicating $H \pm 0.008$.

parameter family, while a one-parameter formulation such as Eq. (1) is used for the mean flow. In addition, a relation between the mean flow and shear-stress parameters is required to close the system of equations. Figure 6 shows typical calculations using the scheme of Perry *et al.*[80,82] for the evolution of ZPG boundary layers from different initial shape factors H and Reynolds numbers. Figure 6(b) displays the evolution of Π versus Re_θ corresponding to the cases in Fig. 6(a). In this scheme, Π may become a true constant only in the asymptotic limit $\mathrm{Re}\rightarrow\infty$, but the variation at finite Reynolds number is very weak. It is obvious from Fig. 6 that all the different evolution curves converge to a single bifurcation line, which can be regarded as equivalent to the asymptotic curves proposed by Nagib and coworkers to indicate when an evolving boundary layer becomes well behaved. According to Perry *et al.*,[81] the evolution curves in Fig. 6 are still somewhat qualitative as they are sensitive to the choice of κ and of the closure model, which requires high quality experimental data for calibration. With new data it should be possible to resolve the evolution question for boundary layers and, in particular, to consolidate the evolution model of Perry *et al.*[81] and the asymptotic state analysis and correlations of Nagib *et al.*[32]

The challenge in designing any facility or computational domain for boundary layers is to quickly achieve and then subsequently maintain the desired pressure gradient for a sufficient distance, while at the same time avoiding the influence of the side and opposite walls. In view of the delicate balance between the wall shear and the growth of the boundary layer at constant pressure, it turns out that the ZPG case is quite difficult to achieve. The model transients presented in Fig. 6 suggest that it can only be approximated experimentally. This observation is augmented by the sensitivity of parameters such as the shape factor H and the von Kármán constant κ to any deviation from the ZPG condition, as shown in the compilation of shape factors in Fig. 7.

III. MEAN FLOW

A. Extensions and alternatives to the logarithmic law

For ZPG turbulent boundary layers and flows in fully developed pipes and channels, the classical arguments lead to a logarithmic variation in the mean velocity profile. Several extensions and alternative formulations have been proposed, but the main alternative is a power-law representation. Before discussing it briefly, however, it is useful to mention two prototypical extensions. The first has been proposed by Wei *et al.*[83] who argued, based on the ratio of viscous and Reynolds stress gradients, that the classical inner and outer layers need to be supplemented by intermediate "mesolayers" (see also Klewicki *et al.*[52]); this is an elaboration of the same concept formulated earlier by Long and Chen,[84] Afzal,[85] and Sreenivasan.[86] In particular, they propose a layer centered on the location of maximum Reynolds stress $y^+_{\mathrm{RS\,max}}$ for which they derive the scaling $y^+_{\mathrm{RS\,max}} \sim (\delta^+)^{1/2}$ in accord with the above references. While these additional layers may help to give a physical interpretation, they do not appear to be necessary in a formal sense because the scaling for $y^+_{\mathrm{RS\,max}}$ is simply the intermediate scaling in the procedure of Kevorkian and Cole[87] for matching *two* layers, that is, the classical inner region and the outer wake region.

A second type of extension has been proposed by Wosnik *et al.*[88] for pipe and channel flows. Using near asymptotics with the friction velocity as the outer velocity scale, they derived a log law, albeit with an extra additive constant for y^+ and a weak Reynolds number dependence for κ, which corresponds, at least qualitatively, to the variation seen in some experiments at low Reynolds number. Regarding the additive constant in the logarithmic profile, B, it must be considered as a higher order correction integrated into the leading order logarithmic profile. Since the logarithmic part of the velocity profile is centered on y^+ of order $\mathrm{Re}_{\delta^*}^{1/2} \gg 1$ (see above), $\ln(y^+ + a^+)$ can be expanded as $\ln(y^+) + (a^+/y^+) + O(1/y^+)^2$. In other words, while such a shift of origin may improve the fit at low Reynolds numbers, it most likely represents only part of the complete higher order correction. Other studies have also noted the possibility of a log law with a shifted origin, including Oberlack,[89] Lindgren *et al.*,[90] and Spalart *et al.*[91]

Returning to the power-law alternatives, Barenblatt[92] showed that if Reynolds number effects persist at all Reynolds numbers the similarity is incomplete and, as a consequence, the mean velocity follows power laws with Reynolds-number-dependent exponents for pipes and channels, and (with further attributes) also in boundary layers. He also remarked on physical mechanisms that could bring about this persistent dependence on viscosity even in the outer layer. These studies have been discussed at some length, and we will not directly add much to that discussion. George and Castillo[51] and George[93,94] argued that the scaling behavior in boundary layers is different from that in pipes and channels since the boundary layer is not homogeneous in the streamwise direction with the consequence, among others, that there is no justification for using the friction velocity as the velocity scale for both the inner and outer regions. In developing an alternative scaling, George and Castillo[51] suggested the *asymptotic invariance principle* that requires a consistent scaling of the equations at all Reynolds numbers. Therefore, based on the asymptotic behavior of the mean momentum equation and requiring a similarity solution for $\mathrm{Re}_\tau = \delta^+ \to \infty$, they conclude that U_∞, the freestream velocity, is the only theoretically acceptable velocity scale for the outer region. This leads to a power-law representation for the mean flow. Recently Jones *et al.*[95] have challenged the assertion that U_∞ is the only acceptable velocity scale using theoretical arguments and show that U_τ is equally acceptable in the asymptotic limit. Also, arguing along the lines of Panton,[96] the outer expansion of the mean velocity $U_{\mathrm{outer}} \sim U_\infty + O(U_\tau)$ should be made nondimensional with U_∞ to yield $U/U_\infty = 1 + O(1/U_\infty^+)$. While this is so far equivalent to the classical formulation, it may be helpful for future theoretical developments.

The debate over power law versus log law may continue until very clear differences can be shown in high-fidelity experimental data at high Reynolds numbers. The real difficulty is that experiments are unlikely to ever reveal asymptotic conditions for a boundary layer. Indeed, one can evaluate the viability of an asymptotic theory only in the context of finite-Reynolds-number corrections, which no theory has satisfactorily produced thus far. For example, the asymptotic limit corresponds to $U_\infty^+ \to \infty$, while for the ASL typical values are $U_\infty^+ = 40$ (and for a boundary layer that is marginally past transition $U_\infty^+ \approx 18$). Hence, for incompressible flows $U_\infty^+ \to \infty$ quickly requires a boundary layer of intergalactic reach, and the limit is practically irrelevant. Nevertheless, a mathematically sound description of the turbulent boundary layer should be well behaved in the asymptotic limit. Recent efforts by Monkewitz *et al.*[49] tackle this problem by considering the self-consistency of leading order terms in asymptotic expansions and finding clear support for the classical scaling and the log law. Monkewitz *et al.*[76] also compared a multitude of high-Reynolds-number experimental data to the classical scaling and the two main power-law theories and conclude that the log law is empirically superior.

B. Asymptotic regime

The issue considered here is the minimum separation of scales required in practice for the mean flow to reach a canonical asymptotic state. It is clear that there is strictly no threshold value, but that the problem needs to be posed as follows: for the asymptotic state to be approached within a preset allowable accuracy, the scale ratio has to be above a certain number. Within the classical framework, this question has become almost synonymous with determining the minimum Reynolds number required to observe a clear logarithmic variation in the profile, which in turn is closely related to the question of the extent of the logarithmic layer. Given Eq. (1), the log law should begin at a fixed value of y^+, while the experiments in Table I give estimates between 100 and 600. In ZPG boundary layers, the extent of a clear log law estimated by Nagib *et al.*[32] from recent experimental data is $y^+ \gtrapprox 200$ and $y/\delta \lessapprox 0.12$. Recent analyses have suggested that the start of the log law may depend on Reynolds number or flow conditions, as discussed below. Wosnik *et al.*[88] concluded that a mesolayer exists in the range $30 < y^+ < 300$ where there cannot be sufficient scale separation to reach high-Reynolds-number characteristics. Lindgren *et al.*,[90] following the Lie group analysis of Oberlack,[89] proposed that no log law exists for $y^+ < 200$ owing to an offset in y.

A rather different estimate has been extracted by Zagarola and Smits[30] and McKeon *et al.*[54] from the very high-Reynolds-number experiments in the Princeton Superpipe. They suggested that a self-similar log region was observed only for $y^+ \geq 600$ and $y/R \leq 0.12$ (with a power-law region for $y^+ < 600$), corresponding to a minimum Reynolds number $\mathrm{Re}_\tau > 5000$. This Reynolds number signaled a sufficient scale separation for a consistent scaling of the pipe friction factor, collapse of the streamwise fluctuations in outer scaling, and the attainment of a constant ratio of the so-called Zagarola and Smits outer velocity scale to the friction velocity, $\xi = (U_{CL} - \bar{U})/u_\tau$ (see Fig. 8). However, it should be noted that the distinct transitions in behavior observed in the Superpipe have not been replicated in other flows (which, however, do not span the same Reynolds number range). Thus, some questions as to the nature of these changes still remain unanswered, and for this the planned CICLoPE experiments will be very valuable.

An alternative place to search for log laws is in the DNS data. Recent advances have seen channel simulations exceed $\mathrm{Re}_\tau = 2000$ (Hoyas and Jimenez[47]) for large box domains ($8\pi\delta$ in the streamwise direction). Jimenez and Moser[98] considered the mean velocity scaling for a range of Reynolds numbers and concluded that no clear log law exists at these

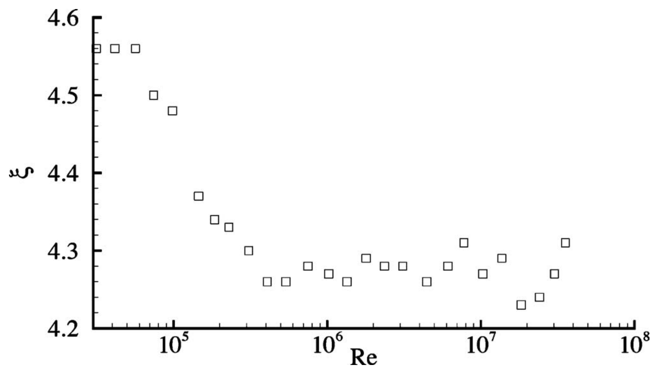

FIG. 8. Variation of the ratio of the Zagarola and Smits outer velocity scale to the friction velocity, $\xi=(U_{CL}-\bar{U})/u_\tau$, with Reynolds number in pipe flow, from McKeon (Ref. 97).

Reynolds numbers. However, by comparing their data to the log law including finite Reynolds number corrections based on a matched asymptotic analysis (such as those described in Afzal[99] and Panton[96]), they concluded that an overlap region may exist for $y/\delta < 0.45$ and $y^+ > 300$. This discussion emphasizes that a lower boundary y^+ for the log law (or its alternatives) is to be regarded only in an asymptotic context as a large number whose numerical value depends among other things on the desired accuracy.

These numerical simulations and recent experiments have shown that it is essential to have sufficiently high Reynolds number before one can actually *see* a log region or any other asymptotic behavior of boundary layer parameters. It is still not entirely clear how high it must be, or whether the answers depend on development length or evolution history. Based on a survey of the available data for different flows, a reasonable estimate seems to be a nominal Re_τ in excess of 4000–5000, although to see a decade of logarithmic variation may require Re_τ in excess of 40 000–50 000.

There remains the issue of how to compare turbulent boundary layers with pipe and channel flows. Most often comparisons are made on the basis of $Re_\tau = \delta^+ = R^+$, where R is the pipe radius or the channel half-height. However, in the boundary layer the flow is essentially nonturbulent for $y > \delta$, while it is turbulent for $y > R$ in the pipe and channel. Therefore, one would expect that the centerline of a pipe or channel $y^+ = R^+$ corresponds to a location $y^+ < \delta^+$ well within the flat-plate boundary layer. To make progress, one may consider the location of the maximum Reynolds shear stress in pipes and channels, $y^+_{\mathrm{RS\,max}} \approx 2(Re_\tau)^{1/2}$ (Sreenivasan[86] and Sreenivasan and Sahay[100]) to the one in ZPG boundary layers, $y^+_{\mathrm{RS\,max}} \approx 2(Re_{\delta^*})^{1/2}$ (Monkewitz and Nagib[101]). This suggests that $R^+ \equiv Re_\tau$ in pipes and channels should possibly be compared to Re_{δ^*} and not δ^+ in ZPG boundary layers. This is equivalent to saying that the physically appropriate outer scale in the boundary layer is the Rotta–Clauser scale $\Delta = \delta^* U^+_\infty$ and not the nominal boundary layer thickness δ, even though the two are asymptotically proportional in the framework of the classical theory ($\Delta/\delta \approx 3.5$ according to Chauhan *et al.*[102]). Hence, the "closeness" to asymptotic conditions in boundary layers and pipes and channels is characterized by Re_{δ^*} and Re_τ, respectively. Some support comes from the estimates of Reynolds number for the mean velocity profile to reach its final self-similar shape: while Monkewitz *et al.*[49] have suggested $Re_{\delta^*} \gtrsim 10^4$ (corresponding to $\delta^+ \gtrsim 2500$) for the ZPG boundary layer, Nagib and Chauhan[103] proposed $Re_\tau \gtrsim 8000$ for channels and pipes. However, it is unclear at this point whether comparisons of boundary layers with pipes and channels are limited in principle.

As has become clear from the above discussions, to resolve questions regarding the extent of the logarithmic layer, it is useful to examine the problem in the framework of matched asymptotic expansions (MAEs), although it is conceded that one needs to assume beforehand the inner and outer scales, and that a choice needs to be made of the gauge functions for the series expansion. The most recent studies of asymptotic expansions are by Panton,[96,104] who examined the mean flow and the Reynolds stresses in wall turbulence. With some assumptions, this analysis gives insights into the inner and outer region interactions. In a MAE approach to the mean flow, the logarithmic profile is the *leading order common part* of inner and outer expansions. Therefore, at any finite scale separation or Reynolds number, this leading order common part will always be contaminated from both sides: from the wall by higher order terms of the asymptotic expansion of the inner mean velocity fit and from the free stream by higher order terms of the expansion of the outer fit. This means that the question of the boundaries of the logarithmic region is ill posed as long as one does not specify what deviation from the exact log law one wants to tolerate. In this sense, if one accepts that the log law is the asymptotic velocity profile in the overlap region, one might state somewhat tautologically that *the log law is always present* even if it is completely overwhelmed by the inner and outer expansions. The DNS of Jimenez and Moser[98] appears to be a case in point.

1. Universality of κ?

The variation of the κ values shown in Table I highlights another unsettled issue that is closely related to the above discussion. Without the results of the Superpipe experiments at the higher Reynolds numbers, and those from wall-bounded flows under a wide range of pressure gradients as summarized by Nagib and Chauhan,[102,103] one may conclude that κ is constant within the uncertainty of measuring wall-shear stress. Such a view is supported by the pipe and channel flow results of Monty,[55] which yielded a von Kármán constant that is identical (within error bars) to the ones extracted from the KTH and NDF ZPG boundary layers (see Table I). Figure 9 shows the hot-wire mean-velocity profiles from Monty[55] on which this conclusion is based. However, we have the view that κ is indeed not a universal constant and is measurably different for different flows.

The view that the von Kármán constant may not be universal emerged from the studies of flat-plate boundary layers with pressure gradient by Nagib *et al.*[106] and Chauhan *et al.*[102] and has been supported by the recent work of Dixit and Ramesh[107] and Bourassa and Thomas.[108] Nagib *et al.*[102,106] advocated that κ is a function of pressure gradi-

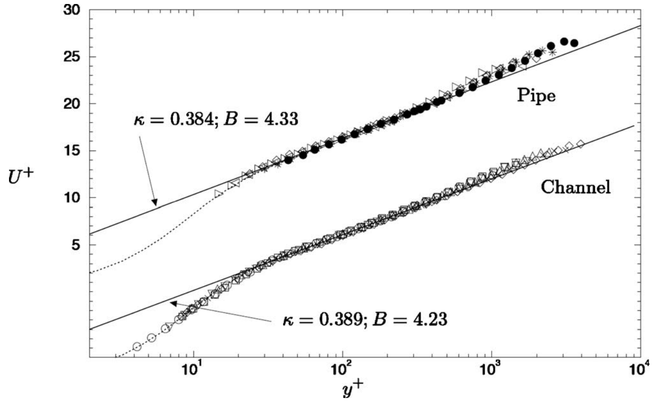

FIG. 9. Pipe and channel flow hot-wire mean velocity profiles of Monty (Ref. 55). Top profiles show pipe flow results: "▷" Re=40 000; "◁" Re=54 000; "◇" Re=69 000; "*" Re=89 000; "●" Re=133 000. Bottom profiles show channel flow results: "○" Re=40 000; "□" Re=60 000; "▽" Re=73 000; "△" Re=108 000; "×" Re=141 000; "◇" Re=182 000. Dotted lines are the DNS data of Spalart (Ref. 105) for the near-wall region only.

ent, noting that this conclusion requires an independent method of determining U_τ. The evidence for this was revealed when equilibrium boundary layers under various pressure gradients were investigated with oil film interferometry and hot-wire measurements at high Reynolds numbers. Figure 10 reproduces some of their results and depicts the variation of skin friction as a function of momentum-thickness Reynolds number for adverse and favorable pressure gradients (FPGs), contrasted with the ZPG case we have focused on here. The trends of the curves in Fig. 10 demonstrate that the von Kármán constant must be different between the three cases with its value largest for the FPG case. Nagib and Chauhan[103] also suggested that κ is different for ZPG boundary layers, pipes and channels. This is based on estimates of κ using composite profiles, and a compilation of data from Nagib and Chauhan[103] is shown in Fig. 11. Since the same asymptotic composite profile without low-Reynolds-number corrections is fitted at all Reynolds numbers, a variation of the fitted κ emerges, as seen on the figure. The idea is that at

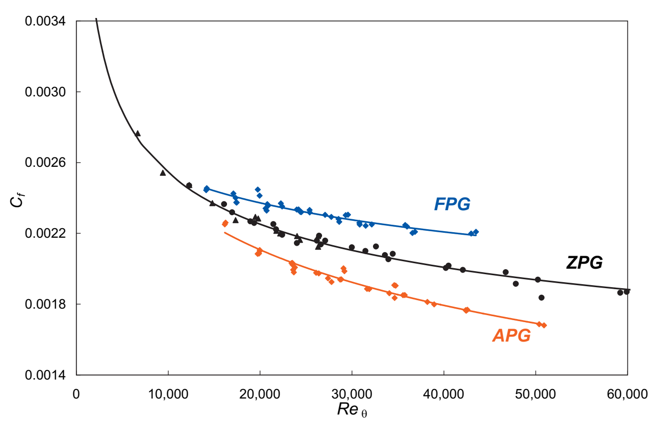

FIG. 10. (Color) Variation of skin friction with pressure gradient for equilibrium boundary layers under favorable (FPG), zero (ZPG), and adverse (APG) pressure gradients; from data of Chauhan and Nagib (Ref. 102).

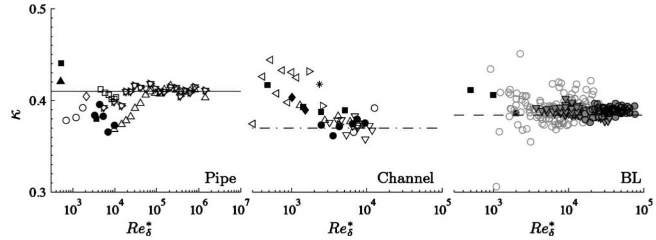

FIG. 11. Nagib and Chauhan (Ref. 103) estimated variation of the κ for in pipes, channels, and ZPG boundary layers obtained using composite profiles. The symbols are as given in by Nagib and Chauhan (Ref. 103) for multiple datasets, including their evaluation of Monty's results (shown with "●" for pipe and channel), together with Superpipe data: "△," Superpipe, static+probe corrected; "▽," Superpipe, static corrected; "▷," Superpipe, uncorrected. "——," κ_P=0.41; "–·–·–," κ_C=0.37; "- - -," κ_{BL}=0.384.

large enough Reynolds number this fitted κ reaches a constant "asymptotic" κ which is then identified with the "true" κ.

The Melbourne pipe and channel experiments[55] involved measurements with hot wires and total-head probes, which were in good agreement after the total-head probe results were corrected for shear effects using the MacMillan[109] correction and for turbulence effects. However, the κ values from the Melbourne pipe and channel are at odds with the values of 0.421 obtained in the Superpipe by McKeon *et al.*[54] and 0.37 in the channel obtained by Zanoun *et al.*[56] In the case of channels, the differences may be due to the role of the aspect ratio of the experimental facilities in the development of the flow and other aspects of determining κ. For the pipe flows, it remains uncertain whether the Reynolds numbers of the Melbourne facility are still too low to exhibit asymptotic behavior. Recall that the Superpipe results suggest a lower end of the log law at $y^+=600$, which corresponds to the outer end of the log layer reported by Monty.[55] The exact asymptotic value of κ extracted by the approach of Nagib and Chauhan[103] for different flows also plays an important role in this discussion of the Superpipe data. As demonstrated in Fig. 11, Monty's results (filled circles) are consistent with κ's extracted from other experiments and DNS; see e.g., the Superpipe values at lower Reynolds numbers. In this regard, one puzzling observation is the trend of the fitted κ with Reynolds number: most of the data appear to approach the asymptotic value from above for boundary layers and channels and from below for pipes.

Further work is needed to explain the above trends and differences, and new collaborative measurement initiatives are underway to address these issues. Since the Superpipe is unique and has produced results at Reynolds numbers far exceeding any previous studies, they have become perhaps the most scrutinized set of experimental data since those of Nikuradse in the 1930s. However, probe corrections pose a challenge. At the higher Superpipe Reynolds numbers the smallest physically practical total head probe has a diameter of several hundred viscous units, which is well outside the range in which the probe corrections have been empirically determined. Also, effects of surface roughness may come into play at Reynolds numbers exceeding 24×10^6. McKeon *et al.*[110] and McKeon and Smits[111] have proposed new, high-

Reynolds-number corrections for both total head probes and the wall pressure tappings that supersede previous methods of measuring the static pressure when probe size becomes a concern. The resolution of the issue of probe corrections is being actively pursued by a multinational measurement collaboration, which includes a comparison between measuring devices with different measuring volumes. Furthermore, an independent confirmation of the Superpipe results is planned in the CICLoPE facility under construction in Italy, which involves fully developed flow in a 0.9 m diameter pipe. The bulk Reynolds number will be nominally limited to 2×10^6, considerably smaller than the 30×10^6 achieved in the Superpipe. Even so, in the CICLoPE pipe the probe size effects will be reduced because of the larger pipe diameter and there is expected to be sufficient overlap with the Superpipe data to allow for rigorous comparisons.

Definitively resolving the issue of whether κ is a universal constant or not requires higher accuracy measurements for both the mean flow and the wall shear stress, coupled with theory-based consistency checks between these two independent measurements. At this point we are leaning toward a flow-dependent κ and note that while some may not consider such detailed arguments about κ very significant, they are crucial to modeling and to numerical simulations of wall-bounded flows. Fundamentally, if κ is indeed variable and depends on the flow and the Reynolds number, it is hardly consistent with a universal logarithmic law.

C. Beyond the mean flow

To close this section, we reiterate that the required accuracy for skin friction and velocity measurements is unrealistically high to fully resolve *all* the above questions about the form of the mean velocity profile. While further high-Reynolds-number experiments are clearly needed, we consider it more promising to move toward theories that incorporate fluctuation statistics rather than dealing merely with the mean velocity, which may well be the least sensitive to Reynolds number variation. Some efforts in this direction already exist, such as the attached eddy hypothesis (Perry *et al.*[67] and Perry and Marusic[112]) and the studies of the streamwise velocity spectra at high Reynolds numbers by McKeon and Morrison[27] and Hutchins and Marusic.[113,114] The latter authors proposed that the appearance of two distinct energy peaks in the premultiplied streamwise velocity spectra, scaling with inner and outer scales, respectively, is a necessary feature of high-Reynolds-number wall turbulence. This spectral peak separation starts to appear for $\mathrm{Re}_\tau \gtrsim 1700$, but these authors proposed a higher limit of $\mathrm{Re}_\tau \approx 4000$ to ensure a sufficient scale separation indicative of high-Reynolds-number turbulence. McKeon and Morrison[27] argued that a similar Reynolds number, $\mathrm{Re}_\tau > 5000$, is required to obtain the scale separation necessary for the existence of both an inertial sublayer in physical space and a spectral inertial subrange, indicative of a fully developed spectrum at small scales, or a decoupling of viscous and energetic scales. It is interesting that these arguments, addressing opposite ends of the scale range, yield a similar estimate for a "high" Reynolds number. It should also be noted that this estimate excludes a large majority of existing studies on wall turbulence from the high-Reynolds-number category.

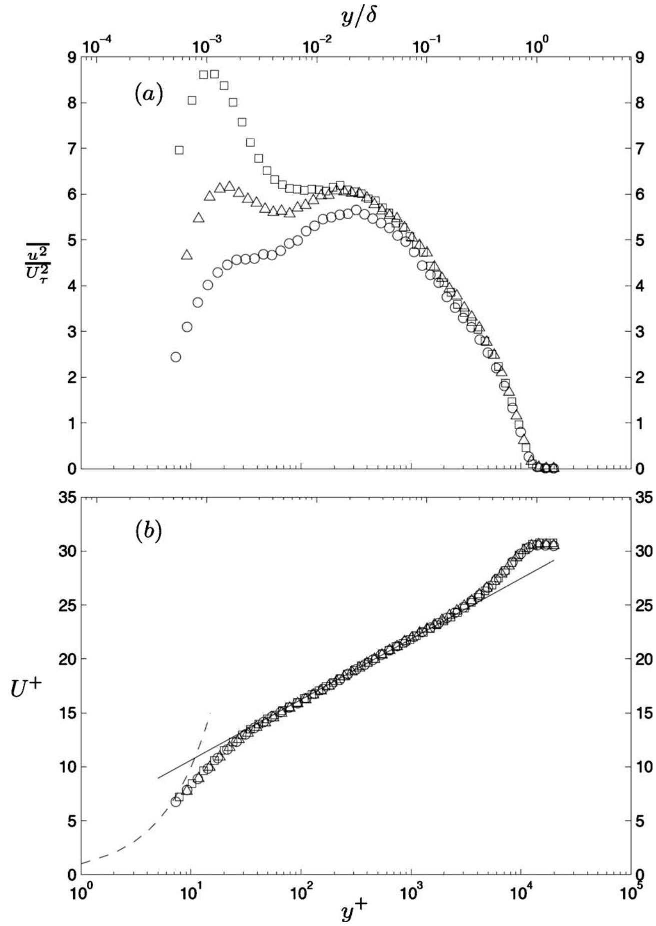

FIG. 12. Streamwise turbulence intensity and mean velocity profiles of Hutchins *et al.* (Ref. 115) measured in the Melbourne wind tunnel at $\mathrm{Re}_\tau = 14\,000$ using different hot-wire sensor lengths: $l^+=22$ (■), 80 (△), and 140 (○).

IV. TURBULENCE INTENSITIES

A. Basic scaling results and spatial resolution effects

While the mean flow field has received the most attention in the past decade, substantial efforts have also gone into understanding the high-Reynolds-number scaling behavior of the streamwise turbulence intensities $(\overline{u^2})$, the corresponding u-spectra, and, to a lesser extent, the other components of turbulence intensity $(\overline{v^2},\overline{w^2})$ and Reynolds shear stress $(-\overline{uv})$. This immediately highlights the challenges facing experiments at high Reynolds number: maintaining adequate spatial and temporal resolution of the probe. Figure 12, taken from Hutchins *et al.*,[115] shows the influence of increasing the sensor length of a hot wire on the measured value of $\overline{u^2}$ and $\bar{U}$. Hutchins *et al.*[115] considered a large number of prior studies and concluded that the attenuation due to finite spatial averaging depends on both the viscous-scaled sensor length l^+ and the flow Reynolds number. For most flows, keeping $l^+ \lesssim 20$ is considered sufficient to resolve most of the kinetic energy in wall-bounded flows (at least for $\overline{u^2}$), but doubts persist below y^+ of 10–20 where the inner maximum of $\overline{u^2}$ is located. Further work is required to firmly establish a guidelines for the maximum allowable l^+ as a function of Reynolds number and wall-normal distance. As yet, no such guidelines are available, and well-established schemes based on assumptions of small-scale isotropy (Wyngaard[116]) are poorly suited to account for the important effect of small-scale anisotropy in near-wall turbulence on spatial averaging.

This issue of spatial resolution has clouded several important trends in the scaling of turbulence intensities, which were referred to in Sec. I (see Figs. 1 and 2). The first is the peak in $\overline{u^2}^+$ that is observed near $y^+ \approx 15$ (as seen in Fig. 12). Surveys of experiments by Mochizuki and Nieuwstadt[117] and earlier studies concluded that this peak in $\overline{u^2}^+$ does not vary with Reynolds number in accord with pure wall scaling, while more recent studies have shown convincingly that the near-wall peak exhibits a weak Re dependence when scaled on U_τ (Klewicki and Falco,[118] Degraaff and Eaton,[36] Metzger *et al.*,[119] Marusic and Kunkel,[20] Hoyas and Jimenez,[47] and Hutchins and Marusic[114]). These later studies (most of which are represented in Fig. 1) took special care to ensure that spatial resolution issues did not influence the results. The second aspect related to spatial resolution has to do with Fig. 2, and with the appearance of a second outer peak or plateau in the $\overline{u^2}^+$ profile at high Reynolds numbers at a wall normal location corresponding to the overlap layer, as reported by Fernholz *et al.*[120] and Morrison *et al.*[22] The prospect of a second outer peak appearing at high Reynolds number would be significant as it may signal the presence of new outer phenomena. However, recent examination of spatial resolution effects suggests that this observation may be affected by spatial attenuation of the hot-wire signal, at distances much further from the wall than previously thought possible (Hutchins *et al.*[115]), at least for the Reynolds numbers considered in those studies. Figure 12 gives an example of how the plateau can become a second peak due to insufficient spatial resolution. At this point the highest Reynolds number at which reliable $\overline{u^2}^+$ profiles are available is not high enough to decide whether these profiles will develop a second outer maximum or only a "shoulder."

Another issue requiring clarification, likely related to spatial resolution effects, has to do with the k_x^{-1} law for the u-wavenumber spectrum in the log region (Perry and Chong,[13] Marusic and Perry,[121] and Hunt *et al.*[122]). While this scaling is predicted from dimensional analysis and the attached eddy hypothesis (among other theories), its experimental validation has been elusive. Morrison[123] and Morrison *et al.*[22] question whether complete similarity, required for the dimensional analysis arguments to hold, can ever be obtained. Alternatively, Nickels *et al.*[35] have reported experimental evidence for a modest k_x^{-1} range, provided that $y^+ < 2\ \mathrm{Re}_\tau/105$ and $\mathrm{Re}_\tau > 5250$. This requires one to be quite close to the wall in units of the boundary layer thickness and at a sufficiently high Reynolds number to ensure that the measurement location is still in the log region. These conditions are particularly difficult to realize, making a k_x^{-1} region of even one decade hard to attain. While the shape of the spectrum dictates that there will always be a tangent with a k_x^{-1} slope, the evidence suggests that the increasing influence of the large scale motions (LSMs) confines self-similar, Reynolds-number-independent k_x^{-1} scaling to limited ranges in physical and spectral space. Note, however, the suggestion of Davidson *et al.*[124] that a relatively extended log variation of the streamwise longitudinal structure function, the spatial equivalent of the spectral k_x^{-1}, can be observed due to the insensitivity of this measure to finite Reynolds number.[125] The issue is further complicated by potential spatial averaging of hot-wire probes: Hutchins *et al.*[115] found that spatial averaging can take place even in the k_x^{-1} region. For example, a 1/3 decade of k_x^{-1} at $\mathrm{Re}_\tau = 14\,000$ with a hot wire of $l^+ = 22$ is found to disappear if a hot wire of $l^+ = 79$ is used. Such restrictions at very high Reynolds number remain a significant challenge for future experiments. An additional complication for inferring scaling laws in spectra, such as k_x^{-1}, is the uncertainty related to using Taylor's hypothesis to convert frequency to wave number spectra. Subtle, but clear, differences are noted between experimental data and those from DNS (Jimenez and Hoyas,[126] Monty and Chong,[127] and Spalart[105]), and further work is needed to resolve these issues.

The scaling of the turbulence intensity profile in the outer region $(y/R > 0.1)$ has received less attention and should be less contentious since resolution effects are minimized far from the wall. For this region, McKeon and Morrison[27] have reported that $\overline{u^2}^+$ profiles as functions of y/R collapse in pipe flow, but differently for high and low Reynolds numbers. They related this phenomenon to the relatively slow development of self-similarity of the spectrum. The latter is characterized by approximate Reynolds number independence of the large scales and the emergence of a $k_x^{-5/3}$ scaling region at high $k_x y$, both of which occur only for $\mathrm{Re}_\tau > 5000$ in the Superpipe data. The authors further speculate about parallels to the "mixing transition" seen in free-shear and other flows for $\mathrm{Re}_{\delta *} \gtrapprox 10^4$ (Dimotakis[128]). This transition has, however, not been observed in other wall turbulence studies, but McKeon and Morrison[27] noted the correspondence with the $\mathrm{Re}_{\delta *}$ necessary to reach a fully self-similar asymptotic mean velocity profile in the boundary layer, and the similarity with the arguments of Marati *et al.*[129]

For the resolution of many of the above open questions with experimental studies, spatial averaging due to finite probe size has emerged as a major limiting factor, but there is hope on two fronts. Several of the newer experimental facilities are of sufficiently large scale for traditional probes to remain small in nondimensional terms for fully resolved measurements. In addition, microfabrication techniques offer the opportunity for increasingly small measuring elements (Kunkel *et al.*[130]), such as the Nano-Scale Thermal Anemometry Probe (NSTAP) at Princeton currently under development.

B. The challenge to wall scaling

It is appropriate to comment on the status of "wall scaling," which continues to be widely used in practical computation schemes. Wall scaling assumes that the turbulence second order moments and spectra scale only with wall units in the near-wall region (for say, $y/\delta < 0.15$), just like the mean flow. The attached eddy hypothesis suggests otherwise and predicts that while the wall-normal turbulence intensity and Reynolds shear stress ($\overline{v^2}$ and $-\overline{uv}$) will follow wall scaling, the streamwise and spanwise components ($\overline{u^2}$ and $\overline{w^2}$) will not, and depend also on Re_τ. Support for this was given by Spalart[105] based on his DNS results, and also by the experimental studies of Perry *et al.*[67] and Perry and Li.[131] The experimental results presented earlier, on the rise in the near-wall peak of $\overline{u^{2+}}$ with Reynolds number, also clearly suggest a failure of straightforward wall scaling in the near-wall region. Jimenez and Moser[98] considered these issues using DNS and experimental data and concluded that $\overline{u^2}$ and $\overline{w^2}$ do not follow wall scaling; the same has been found for the wall pressure (as also discussed by Morrison[123]) and for the local static pressure (as recently measured for the first time by Tsuji *et al.*[132]). Such results, particularly those for the pressure, remain to be incorporated in turbulence models for wall-bounded flows.

On the other hand, most studies support pure wall scaling for the Reynolds shear stress and $\overline{v^2}$ (Kunkel and Marusic[133] and Jimenez and Moser[98]), but the data are limited. Kunkel and Marusic[133] showed collapse of the v-spectra with inner (wall) scaling over three orders of magnitude in Re_τ by making measurements in the log region of laboratory wind tunnel flows and of the ASL. However, Zhao and Smits[134] made similar two component hot-wire measurements in the Superpipe and suggested that $\overline{v^{2+}}$ and the v-spectra in the log region depend weakly on Reynolds number. Further experimental study is clearly needed to resolve this issue, which is, in particular, relevant to several computational schemes (Durbin and Pettersson-Reif[135]).

The least amount of experimental data exists for $\overline{w^{2+}}$, although its importance should not be underestimated (see, e.g., Lighthill[136]). Jimenez and Hoyas[126] reviewed most of the existing experimental studies and showed detailed comparisons of all components of spectra and cospectra for DNS of channel flows studies up to $Re_\tau=2000$. They find that the large outer motions of the spanwise and wall-normal velocities in boundary layers are stronger than those found in channel flows, but conclude that qualitatively similar outer-layer structures seem to exist in channels, pipes, and boundary layers at high Reynolds numbers. Recently, the available data were also surveyed by Buschmann *et al.*[137] who concluded that clear quantitative differences of $\overline{w^{2+}}$ and $\overline{v^{2+}}$ profiles exist between boundary layers, pipes, and channels.

V. STRUCTURE OF THE TURBULENCE

Alongside the studies of the scaling of turbulent statistics, significant effort has been invested in unraveling the nature of organized motions in instantaneous velocity fields. Our current understanding of coherent structures will be explored first before discussing the VLSM mentioned earlier.

A. Coherent structures

Despite the consensus that coherent structures provide important clues to understanding wall turbulence, considerable controversy remains as to what the coherent structures are, and what specific roles they play. In general terms, we may regard coherent structures as organized motions that are persistent in time and space and contribute significantly to the transport of heat, mass, and momentum. The mechanisms for the sustenance of wall turbulence need to be related to these structures, and a large number of scenarios have been proposed to describe these time-dependent interactions (Panton[17]). The views on these interactions may be loosely classified into two broad classes. One view is based on instability and transient growth mechanisms principally in the inner region, and the other on vortex-structure regeneration mechanisms. An example of the latter is described by Adrian,[18] where hairpin-type vortices are regarded as the fundamental building blocks for describing the physics. An example of the first line of thinking is the view of Schoppa and Hussain[138] that complete hairpin vortices do not exist in wall turbulence.

This dichotomy is likely to persist for several reasons, one of which is that there is at present no universal definition for what constitutes a coherent structure and, in particular, a vortex, thus making meaningful comparisons difficult (although with the work of Chakraborty *et al.*,[139] a consensus may be emerging). Furthermore, even if such a definition is agreed upon, detailed information is required on the time-evolution of vortex structures, and this has not yet become available. DNS would seem the ideal tool to obtain this information, but even here considerable differences are noted. For example, Schoppa and Hussain's DNS data show no hairpin vortices, while in recent DNS of a spatially evolving boundary layer, Wu and Moin[140] found a striking predominance of clearly defined hairpin vortex structures. As discussed by Marusic,[141] it is not clear what role the specific details of the numerical schemes and specification of inlet boundary conditions play in the appearance of the vortical structures. Detailed comparisons between recent DNS results for comparable Reynolds numbers, such as those of Wu and Moin,[140] Schlatter *et al.*,[142] Ferrante and Elgobashi,[143,144] and others, should be able to shed light on this difference. The DNS results of Schlatter *et al.*[142] have recently been extended to momentum Reynolds numbers slightly above 4000, demonstrating that as the flow develops further away from the transition region, considerable randomness evolves resulting in a flow which is better represented by the much earlier descriptions of Robinson.[16]

Another issue that confuses the discussion on coherent structures is their relationship to the mean flow (and other statistics). Many studies refer to coherent structures that draw energy from the mean flow, while in the attached eddy modeling work of Townsend[5] and Perry and Marusic,[112] the attached eddies account for the mean flow and the turbulence fields. Furthermore, the eddies in these latter models are statistically representative structures, whose shape does not necessarily correspond to any instantaneous realization.

Notwithstanding the variety of definitions of coherent motions, the study of coherent structures has advanced considerably in recent years. This is largely due to advances in PIV and DNS that have brought increasing insight into the development of spatially coherent, stress-bearing structures that play an important role in transport problems in turbulent boundary layers, particularly in the near-wall region. We shall classify the main coherent structures into three categories: (1) the inner streaks associated with the near-wall cycle with a spanwise scale of $\mathcal{O}(100\nu/U_\tau)$; (2) LSMs of scale $\mathcal{O}(\delta)$; and (3) VLSMs (termed VLSMs by Adrian and coworkers) or "superstructures" (Marusic and coworkers) with streamwise length scales of $\mathcal{O}(10\delta)$.

The near-wall cycle has been extensively explored (for some recent work, see the PIV studies by Kahler[39] and Stanislas *et al.*[145]). The interpretation of LSMs in most studies agrees with Theodorsen's hairpin vortex paradigm. As summarized by Adrian,[18] packets of individual eddies (whose representative form is well described by the hairpin model) that are aligned in the streamwise direction are observed with a packet length scale of the order of δ. The packets appear to be capable of self-regeneration (Zhou *et al.*[146] and Kim *et al.*[147]) and explain the long streamwise correlations and other trends observed in the data (Marusic[28]). Flow visualization and PIV experiments reveal spanwise vortices associated with the hairpin heads, and the so-called retrograde vortices with the opposite sense of rotation (Falco,[148] Smith *et al.*,[149] Wu and Christensen,[150] Natrajan *et al.*,[151] and others). The spanwise growth and extent of the packets have been measured by Tomkins and Adrian,[38] Ganapathisubramani *et al.*,[152] Hutchins *et al.*,[153] and Hambleton *et al.*[41] Associated with the passage of a hairpin packet are wall-normal zones of approximately uniform momentum that persist for a finite time and can be clearly seen in the streamwise velocity signal. However, the observations of hairpins have been confined to low-Reynolds-number flows and their signature was noticeably absent in the surface layer PIV of Morris *et al.*,[154] although spatial resolution may have played a role in that study. There is a question of the robustness of such structures in higher Reynolds number boundary layers with physically larger logarithmic regions, as articulated by Adrian.[18] While the evidence for hairpin packets has come mostly from flow visualizations and spatial PIV images, there is also good evidence of coherence in temporal streamwise velocity signals on the scale of δ and larger.

B. VLSMs

Recent work concerning the VLSMs deserves particular attention as many key questions await answers. It remains, in particular, unclear how similar VLSMs and superstructures are in pipes, channels, and boundary layers. Monty *et al.*[155] compared a channel, pipe, and boundary layer at the same Reynolds number of $\mathrm{Re}_\tau=3000$ and found the VLSM energy in pipes and channels agrees well, but resides in larger wavelengths and at greater distances from the wall than those in boundary layers. Furthermore, for $y<0.5\delta$, while the turbulence intensities are equal, the distributions of energy among the scales are different. This suggests that the VLSMs in all three flows might be similar and only have longer scales for pipe and channel flows. The quantitative differences are likely due to the interaction with the opposite wall in internal flows and the intermittency of the outer region in boundary layers, but remain a matter of speculation. Despite the uncertainty about the origin and scaling of VSLMs and superstructures with streamwise coherence of $O(10\delta)$ and more, we feel that their physical origin is the same and we will treat them here as the same phenomenon.

Figure 4 showed the development of the premultiplied k_x spectrum in pipe flow at the outer edge of the overlap layer, $y/R=0.1$, with increasing Reynolds number. The influence of motions of scale $\mathcal{O}(10\delta)$ are seen to increase with Reynolds number and, at this location, the VLSMs contain significant energy—more than half the total for $\mathrm{Re}_D=\mathcal{O}(10^5)$. By use of a spanwise array of single hot wires and Taylor's hypothesis, Hutchins and Marusic[114] proposed that the true extent of these correlated regions for a boundary layer may be as high as 20δ, but that spanwise meandering or variations in the streamwise/spanwise plane reduce the extent recorded by a point measurement technique. Monty *et al.*[156] performed similar measurements in pipe and channel flows and concluded that the VLSMs in both flows have a similar length, $\mathcal{O}(25R)$ or $(25h)$, respectively, and that their width was found to be about 1.6 times that of similar structures in the ZPG boundary layer. Bailey *et al.*[157] confirmed these conclusions by using temporal correlation data measured in the Princeton Superpipe. This may mean that the largest structures in boundary layers are different in detail from those in channels and pipes (or that δ is not equivalent to R and h as discussed in Sec. III B). That the VLSMs in internal flows may be longer than in boundary layers helps to explain the increased energy at large scales in internal flows (see also Monty *et al.*[155]). Geometrical confinement must play some role in the amplitude of the meander and hence the apparent length of the coherent regions. The implications of these differences for modeling have not been appreciated.

In the DNS of channel flow, Jimenez *et al.*[158] and Jimenez and Moser[98] described the presence of "global" structures that appear to be quasihomogeneous in the streamwise direction and coexist with the so-called autonomous cycle of near-wall turbulence. At the Reynolds numbers typical of DNS, Jimenez and coworkers indicate that the streamwise quasi-independent nature of the large modes means that they can be well modeled in a box size of order 2δ in the streamwise direction, that is, without capturing the full extent of the global structures. There is also some evidence for large roll modes in Couette-flow DNS, although there has been much discussion as to whether these may be a consequence of periodic boundary conditions. Furthermore, the extension of these observations to higher Reynolds number flows is still an open issue.

As VLSMs have come into view only recently, many questions remain open at this time. An obvious first set of questions concerns possible problems with the identification of VLSMs. At these length scales, for example, low frequency fluctuations associated with the facility itself may have an important influence. Estimates of streamwise lengths of VLSM/superstructures is complicated by the fact that their transverse scale is of the order of the thickness of the turbulent layer and their close lateral packing can lead to overestimates in length if neighboring lateral structures are grouped together and interpreted as one (Schlatter *et al.*[142]). Moreover, a considerable amount of quantitative data on VLSM is obtained by using Taylor's hypothesis and from temporal

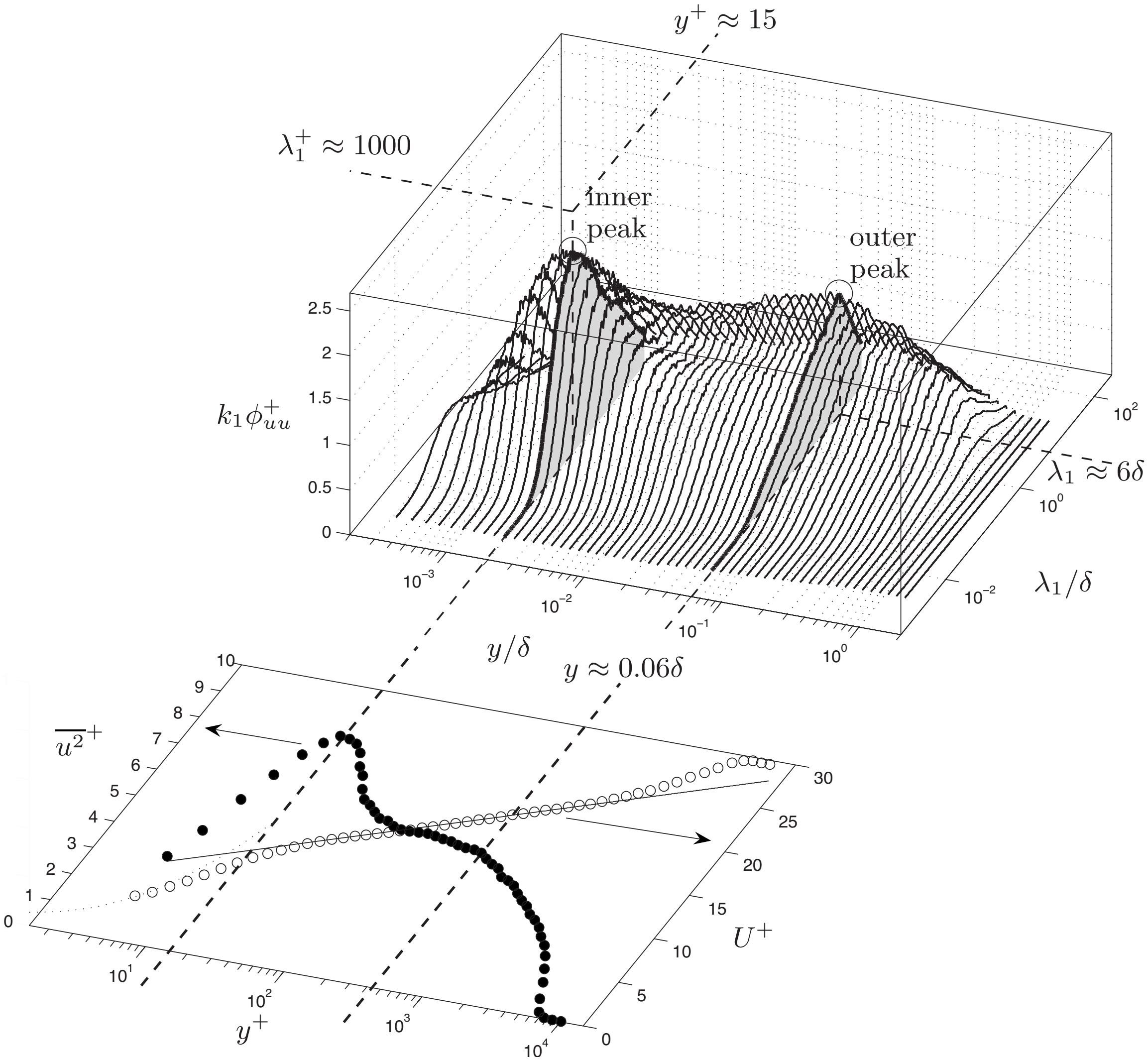

FIG. 13. Inner and outer peaks in spectrograms of fluctuating streamwise velocity in a boundary layer at $Re_\tau=7300$ from Hutchins and Marusic (Ref. 113). The lower plot shows the corresponding mean velocity (open small circles) and broadband turbulence intensity profiles (filled circles) where the dotted line shows linear behavior in the viscous sublayer $U^+=y^+$ and the solid line shows the log law (where $\kappa=0.41$ and $B=5.0$). For all plots, the dashed lines denote locations of inner and outer spectral peaks.

streamwise spectra. However, the validity of Taylor's hypothesis to convert temporal to spatial data remains a cause for concern, particularly since the length of VLSMs typically exceeds the length of the field of view that can be achieved with current experimental diagnostics. Spatiotemporal correlation measurements in boundary layers by Volino *et al.*[159] and Dennis and Nickels[160] indicate the decreasing accuracy of Taylor's hypothesis as the apparent structure size increases. In addition, the channel flow DNS of del Alamo *et al.*[46] has demonstrated that the convection velocity of the longest structures scales with the centerline velocity rather than the local mean. Due to the increasing influence of the VLSMs across the wall layer with increasing Reynolds number and the corresponding increase in velocity difference across a single structure, it is clear that Taylor's hypothesis becomes progressively worse toward the wall. Near-wall ASL measurements by Metzger *et al.*[161] have reinforced this observation.

C. Influence of the superstructures on the near-wall region

At low Reynolds number, the spectral content of the superstructures overlaps with motions corresponding to the near-wall cycle, that is, $10\delta=\mathcal{O}(1000\nu/u_\tau)$. While there has been speculation about this phenomenon since the 1960s, it was documented most clearly by Hites.[162] As the Reynolds number increases, double spectral peaks in the buffer layer and log region emerge, as shown in Fig. 13. Several studies, including Hutchins and Marusic,[114] Jimenez *et al.*,[158] and del Alamo and Jimenez[163] have shown that outer-scale influence on the near-wall region becomes increasingly noticeable with Reynolds number, and this likely leads to the increase in $\overline{u^2}^+$ with increasing Re_τ. Degraaff and Eaton[36] proposed a mixed scaling with $U_\infty U_\tau$ instead of U_τ^2 scaling, and this seemed to produce a good empirical collapse of their $\overline{u^2}$ results. Marusic and Kunkel[20] used an outer forcing on the near-wall

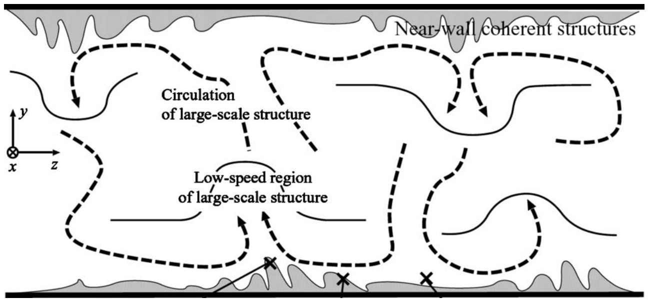

FIG. 14. Schematic taken from Toh and Itano (Ref. 166), showing their interpretation of how the large-scale structures interact with the near-wall eddies in their low-Reynolds-number channel flow.

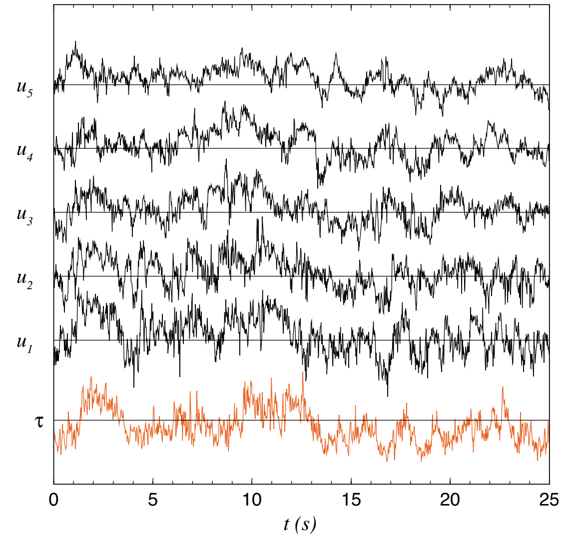

FIG. 15. (Color online) Time traces from Marusic and Heuer (Ref. 169) measured in the ASL at $Re_\tau \sim O(10^6)$. Fluctuating velocities at five wall-normal positions in the log layer are simultaneously shown with the fluctuating wall-shear stress. Significant coherence is noted between the wall shear stress and the velocity signals at this high Reynolds number.

region based on the attached eddy hypothesis of Townsend[5] and predicted that the peak value of $\overline{u^2}^+$ should scale effectively with log Re_τ. Asymptotically this leads to a form close to mixed scaling. However, they emphasized that this should not be interpreted as an outer region scaling on U_∞. The attached eddies all scale with U_τ and it is the distribution of their length scales, and their collective contributions to the near-wall region, that give the Re_τ dependence.

The log Re_τ scaling of the peak value of $\overline{u^2}^+$ is borne out by the results from the smooth-wall ASL results of Metzger and Klewicki,[21] within the estimated experimental error, as shown in Fig. 1. Large uncertainty is associated with the trends reflected in this figure because of the many reasons discussed in Sec. II A, including spatial resolution of probes in the laboratory and the correspondence of the ASL to laboratory boundary layers. What we are confident about is an increasing trend with Reynolds number reminiscent of the slow (but decreasing) trend of the shape factor discussed by Nagib *et al.*[32] While two decades or more of DNS of channel flows did not reveal this important trend, recent computations and asymptotic analysis support it. The impact of such new understanding on the various commonly used turbulence models has not been fully appreciated.

The interdependence of the near-wall production cycle and large scale structures is not a new finding as it was discussed and documented decades ago by Rao *et al.*[164] and Wark and Nagib;[165] the former were interested in Reynolds number scaling issues and the latter in quantitative description of the large structures through careful experiments. DNS studies by Spalart,[105] Abe *et al.*,[44] Toh and Itano,[166] Iwamoto *et al.*,[45] and Hoyas and Jimenez[47] have also noted the influence of LSMs at the wall. A schematic interpretation of Toh and Itano is shown in Fig. 14. Although their simulations were done at very low Reynolds number and with short streamwise boxes, the cartoon in Fig. 14 gives a good representation of the nature of the interaction supported by other studies. Hutchins and Marusic[113,114] showed clear evidence of the "footprint" of the superstructures on the near-wall flow in instantaneous time series and spatial data. Moreover, by examining low-pass filtered, fluctuating streamwise velocity time series, they reveal that the interaction strongly resembles an amplitude modulation of the small scales by the large scales. Near the wall, small-scale turbulent activity in all components of the Reynolds stress is seen to be relatively suppressed during a large-scale negative velocity excursion (with the opposite being true during large-scale positive velocity excursions), while further from the wall the relationship reverses. The increasing importance of this nonlinear interaction, across very large to small scales, poses several difficulties for the interpretation of the harmonic spectral decomposition of temporal signals. As such, alternative methods of analysis, including the Hilbert transform, have been explored recently (Tardu[167] and Mathis *et al.*[168]). Synchronous measurements across the wall region indicate a large wall-normal extent of the footprint, extending from the log region to the wall, thus influencing the fluctuating component of the wall shear stress. Recent DNS results by Schlatter *et al.*[142] show strong evidence of this feature (see also Abe *et al.*[44] and Hu *et al.*[48]), and the outer influence is seen to increase in strength as the Reynolds number increases (Hutchins and Marusic[114]). An example of this influence at very high Reynolds number is shown in Fig. 15, taken from Marusic and Heuer.[169] The velocity signatures shown in the figure are all from the log region and significant coherence is noted between the velocity signals and the wall-shear stress signal.

In the final analysis, the origin and wall-normal extent of the VLSMs at high Reynolds number and the locus of the distinct outer peak that emerges in the logarithmic region remain to be determined. The linear stability analysis about a turbulent mean profile constructed using an eddy viscosity by del Alamo and Jimenez[170] reveals clear evidence of two highly amplified spanwise wavelengths for long streamwise structures, one scaling on inner variables and one on outer variables, perhaps providing a clue to the origin of the VLSMs. Recently, Mathis *et al.*[168] investigated the location of the outer spectral peak and found that it nominally follows the geometric center of the logarithmic region, coinciding with the reversal of the phase relationship between large-scale and small-scale turbulent intensities. However, at this stage of our understanding, firm conclusions on the correct scaling of these phenomena remain elusive. In this context it is finally also worth mentioning that Pujals *et al.*[171] and Cossu *et al.*[172] have found very large transient amplification of extremely large streaky structures with transverse wave lengths of the order of several h or δ both in the channel and boundary layer. It is not clear whether such structures are actually excited naturally but they might well have escaped current experimental diagnostics because, generally speaking, streaks occupy a strange position somewhere between mean flow and turbulence: if one pins them down (which is easy to do experimentally with periodic roughness elements, at least at lower Reynolds numbers) or if their width is larger than the meandering amplitude, they appear as a steady mean flow distortion. They become turbulence only if they meander.

Adrian,[18] Guala *et al.*,[173] and Balakumar and Adrian[29] have reported that, while there is no evidence of extremely long scales in the wall-normal velocity spectra due to the presence of the wall, the superstructures must be considered to be "active" in the sense that they bear a significant portion of the shear stress. As noted by Jimenez and Moser,[98] while experiments and computations have illuminated the kinematics of the log layer, further advances will be required to describe the dynamics in detail.

VI. ROUGHNESS

Interest in surface roughness effects on wall turbulence has grown over the past few years, partly because with increasing Reynolds number even the most well-controlled surface will appear rough as the viscous scale becomes sufficiently small. Flows with rough walls are more likely to be observed in an applied setting, and in experimental terms a special effort is required to control surface roughness for purposes of exploring scaling in the smooth-wall case. However, our state-of-the-art understanding of rough-wall flows still does not permit an *a priori* prediction of the influence of a surface roughness on the quantity of most practical interest, the skin friction, even in the case when the roughness length scale distribution has been fully characterized (by either k_s, the equivalent sand-grain roughness height, or k, the rms roughness height). A comprehensive review of rough-wall turbulence was recently given by Jimenez.[174]

The classical notion, spelled out explicitly by Townsend, is that the influence of surface roughness on the outer flow is confined to a change in boundary condition through the friction velocity. A key assumption here is that the Reynolds number δ^+ is sufficiently large that a significant k^+ can be achieved with small k/δ in order to maintain the integrity of the outer flow. Recent studies at high Reynolds numbers have tended to confirm this result, even for large roughness with an upper limit of order $y/\delta=0.1$ (Allen *et al.*[175] and Flack *et al.*[176]). In this respect the experiments by Krogstad and Antonia[177,178] that showed an effect of roughness on the outer flow seem to be an anomaly, although this may be due to the use of two-dimensional roughness (see below). Experiments in the Superpipe indicate that the mean velocity and turbulent intensities in the outer region of high-Reynolds-number pipe flow scale in the same way as smooth wall data, with the same value of κ obtained for the log region (Allen *et al.*[175] and Shockling *et al.*[179]). Boundary layer experiments by Flack *et al.*[176] have demonstrated that the effects of roughness extend to about three times the equivalent sand-grain roughness height, potentially destroying, or at least modifying, the near-wall cycle. Interestingly, high-Reynolds-number results from the near-neutral ASL from several authors (Hommema and Adrian,[180] Hutchins and Marusic,[114] Morris *et al.*,[154] extensive earlier literature on laboratory boundary layers) indicate that large-scale motions and the uniform momentum zones associated with inclined hairpin packets at lower Reynolds number develop even if the surface is not hydrodynamically smooth. However, the reduction of the near-wall turbulence intensity peak (e.g., Metzger *et al.*[161]) within the roughness-affected layer of the flow suggests a decoupling of the near-wall stress-bearing motions from the outer motions relative to the smooth-wall case, which requires the "top-down" influence discussed earlier, even over a rough wall. In contrast to this view, Morrison[123] pointed out that Townsend's hypothesis is essentially a condition of no interaction between inner and outer regions. This requires further investigation in light of the results for smooth walls discussed above.

Flow response to small roughness amplitudes has been a topic of particular importance to the interpretation of results from the Superpipe. While several authors (e.g., Barenblatt *et al.*[50] and Perry *et al.*[181]) have attributed the unique mean velocity results from this facility to a surface that is transitionally rough at high Reynolds numbers, recent analysis with high-Reynolds-number probe corrections (McKeon *et al.*[54]), together with the more recent studies of controlled roughness in the same facility, has confirmed that the original smooth pipe should be considered to deviate from a hydrodynamically smooth condition only for Reynolds numbers larger than $Re_D \approx 20\times 10^6$. Schultz and Flack[182] measured a similar honed-surface roughness in their boundary layer facility and found the same Hama roughness function measured by Shockling *et al.*[179] in the Superpipe using an exaggerated form of the roughness present in the original "smooth" pipe investigations by Zagarola and Smits[30] and McKeon *et al.*[54] Importantly, the form of the Hama function for small roughness appears to be nonuniversal, in contrast to the accepted wisdom that there is an absolute threshold in equivalent roughness amplitude, k_s^+, below which the surface may be considered hydrodynamically smooth with the smooth wall value of the additive log-law constant B. For some types of roughness, such as honed surfaces (Shockling *et al.*[179]) and commercial steel pipes (Langelandsvik *et al.*[183]), the onset of roughness is well defined, but this behavior is not universal (see, for example, the data of Colebrook[184]). Certainly the exact form of the Hama function must be treated as specific to the roughness geometry. Further study is merited.

The rough-wall pipe studies by Shockling *et al.*,[179] Allen *et al.*,[175,185] and Langelandsvik *et al.*[183] permit the generation of universal resistance plots in the style of the well-known

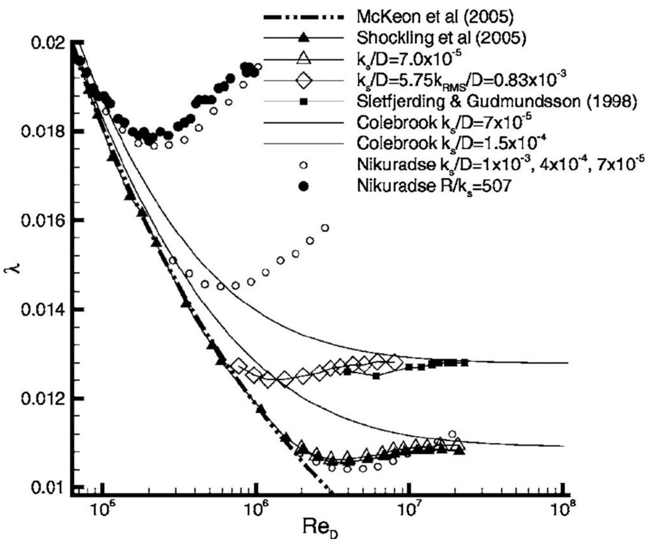

FIG. 16. New universal resistance plot for honed surfaces, taken from Allen *et al.* (Ref. 185). This is an alternative to the Moody diagram for this type of roughness. Symbols and references as given in Allen *et al.* (Ref. 185).

Moody plot for various roughness distributions. The result for a honed pipe[185] is shown in Fig. 16. In contrast to the behavior seen in the Moody plot, the friction factor in the transitionally rough regime follows an inflectional sand-grain-roughness-type distribution rather than the monotonic Colebrook[184] relationship. Contrary to the previously accepted wisdom, this trend has been found to be common to most roughness types. The trend also agrees with the results of the semiempirical model of Gioia and Chakraborty[186] in which the inflectional "trough" is associated with increased shear stress at the scale of the roughness elements. One roughness type that does not follow this inflectional trend is the commercial steel pipe roughness studied by Langelandsvik *et al.*[183] The results showed a monotonic change from smooth to fully rough behavior, which occurred over a very much smaller Reynolds number range than the Colebrook correlation would indicate.

Without further theoretical advances, there is a risk of needing a "catalogue of roughness results" to account for the continuum of roughness distributions observed in practice. In light of recent advances in the near-wall structure of smooth-wall flows, there is a pressing need for further investigation of the rough-wall case.

From the above discussion it is evident that the main complication when discussing rough walls is the geometry of the roughness. Two-dimensional roughness (for example, spanwise rods) has been shown in the experiments by Krogstad and Antonia[178] and in the simulations by Lee and Sung[187] not to follow Townsend's hypothesis for flat-plate boundary layer flows, with significant differences in the outer flow when compared to smooth walls and to walls with three-dimensional or random roughness. This is not the case in channel flows where two-dimensional roughness does not lead to a violation of Townsend's hypothesis (Krogstad *et al.*[188]). The reasons for the differences remain unclear, although it is suspected that in pipes and channels the imposed linear shear stress profile may be inhibiting the differences. Whether two-dimensional roughness in unconfined flows is the only anomalous case is unknown at present.

VII. SUMMARY AND CONCLUSIONS

In this section the main topics of the previous sections are summarized, with some additional comments and conclusions as appropriate. We also emphasize topics and findings that have not yet found their way into textbooks or recent reviews.

A. Log law

For the new data discussed here, the log law remains the preferred description of the mean velocity profile in wall turbulence. However, the universality of its parameters and the extent of the logarithmic overlap region have been a subject of debate.

First, recent high-Reynolds-number research has indicated that the viscous influence extends farther from the wall than previously understood. According to textbook wisdom the logarithmic profile starts at $y^+=50$, or even 30. Experimental estimates of the wall distance beyond which a log law is discernible range from $y^+ \gtrsim 200$ in boundary layers to $y^+ \gtrsim 600$ in the Superpipe at very high Reynolds number. It is an open question whether this lower limit is a function of Reynolds number and/or whether these discrepancies can be attributed to inadequate probe size in the Superpipe experiments at the high-Reynolds-number end or other ambiguities in the interpretation of data.

Second, the best estimates for the log-law constants, which incorporate the highest-available Reynolds number for each flow, appear to depend on the flow type. For pipe flow the constants appear to be $\kappa=0.42$ and $B=5.6$, but data for this are limited. For the ZPG boundary layer, a wide range of facilities provide confidence that κ is between 0.38 and 0.39 and the additive constant is 4.2. For channel flows we have more uncertainty in the value of κ as it ranges between 0.37 and 0.39, but it is clearly less than the most widely used value of 0.41. These results reaffirm the conclusion that the value of $\kappa=0.41$, adopted since the 1960s and extensively used in modeling, and even in experiments without independent wall-shear measurements, is not the correct value. These are subtle points, but the differences being considered are also subtle. To move toward their resolution, it is evident that a framework such as MAEs, in particular, a uniform determination of all mean flow parameters from fitted composite profiles, would be very beneficial. The challenge will be to develop a theoretical underpinning for the composite profiles that are used. What is perhaps worth mentioning is that the skin friction measurements seem to have advanced to a point where small differences in κ can be discussed seriously, instead of putting them under the vague category of being within experimental uncertainties.

Whether these problems suggest a need to extend the log-law analysis by interposing further layers (Klewicki *et al.*[52]) or that a deeper change is required (as has been advocated by Barenblatt[92]) is not completely clear. One should also not forget that the skin friction or U_∞^+, the shape factor H, and the streamwise boundary layer growth $\delta^*(x)$ are intimately tied to the parameters of the mean flow profile (Monkewitz *et al.*[49]) and therefore provide useful cross-checks on consistency. Similarly, in internal flows, consistency is required between the mean flow parameters and the profiles in inner and outer scaling, the centerline velocity, the friction factor, etc. (McKeon *et al.*[54]). Additional high-Reynolds-number experiments, and even more accurate skin friction data, would be valuable in these regards. If the log law is indeed the proper asymptotic solution, determining the von Kármán "constant" from first principles represents a grand challenge for our field. Having different values of κ for ZPG boundary layers, pipe, and channel flows presents a significant challenge for turbulence models, as well as theory.

B. Relation between inner and outer scaling

Evidence of outer-scale contributions to the near-wall region has been noted since the study of Rao *et al.*,[164] who documented that large outer-scaled structures were active in rearranging and interacting with near-wall structure, and consequently influencing the "bursting" frequency. Recent studies show that such inner-outer interactions become more evident with increasing Reynolds number, particularly for the streamwise component of turbulence intensity. This contradicts wall-scaling approaches that assume all inner region statistics to scale exclusively on inner variables. While the location of the near-wall peak of $\overline{u^2}^+$ scales with inner variables, in boundary layers there is a clear trend of increasing magnitude with Reynolds number. On the other hand, the spacing of near-wall streaks is found to be independent of Reynolds number over a very wide range when scaled on inner variables. Mixed scaling (a geometric mean of inner and outer scales) does not seem to provide a physically meaningful scaling parameter given the complexity of the interactions. Present data also suggest that the peaks in $\overline{w^2}^+$, and possibly in $\overline{v^2}^+$, change with Reynolds number in location and value (as previously reported by Sreenivasan[15]). Despite the uncertainties of present data, it is difficult to escape the conclusion that different components of the Reynolds stress tensor scale differently. This poses a problem of mathematical consistency as one expects a tensor to scale as a whole. A "way out" may be the concept of block matching (Crighton and Leppington[189]) in MAE in which all the terms with the same power of the small parameter ϵ multiplied by any power of $\ln(\epsilon)$ are considered to be of the same order. Applied to the Reynolds stress tensor, a slow growth of some of its components as $\ln^n(R)$ would be mathematically describable. It is increasingly likely that for each inner (outer) quantity there exists an essentially inner (outer) scaling modulated by some weak function of Reynolds number, and the extent of this modulation will depend on the quantity that is being considered. Again, these issues will remain open until detailed measurements are carried out over a range of Reynolds numbers up to some very high value and/or a coherent theoretical framework is put forward.

C. Turbulence structure

We noted three basic eddy motions: near-wall streaks, which have been shown to follow inner scaling, the LSMs, which are related to outer layer bulges and the vortex packets as discussed by Head and Bandyophadyay[12] and Adrian,[18] and the VLSMs interpreted by Adrian and coworkers in terms of concatenated packets of vortices and by Marusic and coworkers in terms of the meandering superstructures. Separation of the latter two structure types is nontrivial since their very nature dictates that Taylor's hypothesis cannot be appropriate as a diagnostic tool. Although this conclusion has been widely accepted in the past, recent measurements in the near-wall region have added significance to this observation. An important consequence of the interaction between these structures is observed via the Reynolds-number-dependent peak of the streamwise intensity in the inner layer (near $y^+ = 12-15$).

While large streamwise structures in wall turbulence have been documented for many decades (Townsend[4] and Kovazsnay *et al.*[190]), the dynamical importance of the largest structures (VLSM) had not been appreciated until recently. For example, the low wavenumber VLSMs appear to contribute about half of the total energy of the streamwise turbulence component at high Reynolds number. Also, they do not appear to scale with outer layer variables as assumed in the Perry–Townsend attached eddy model. What is clear is that differing views exist and many open questions remain regarding the VLSM/superstructures. One key question concerns their scaling. If they depend on the scale of the apparatus, it suggests the disturbing and profound possibility that it is not possible to realize a facility-independent asymptotic state of turbulence (even for fully developed internal flows, such as pipes and channels).

The role of the turbulence structure relates directly to the spectral scaling laws. While $k_x^{-5/3}$ scaling in the spectrum of the streamwise component is well established, experiments now indicate that the k_x^{-1} region is only evident at very high Reynolds numbers over a very limited wave-number range. Although the interactions between outer layer motions and inner layer motions have become much clearer in recent years, the simple division between inner and outer layer scaling that leads to the k_x^{-1} region fails to capture those interactions. Specifically, the region where we might expect k_x^{-1} scaling corresponds to the wave numbers occupied by the LSMs, and experiments have shown that although the LSMs appear to behave as attached motions, they do not scale simply on wall variables.

D. Boundary layers versus pipes/channels

We mentioned the puzzle as to whether the von Kármán constant κ is different in pipes, channels, and boundary layers. Other differences have also been highlighted between boundary layer flows and the confined flows of pipes and channels. This extends beyond the well-documented and obvious differences in the outermost region and includes the inner-scaled streamwise turbulence intensity and the other components of Reynolds stress, which may be subtly different between these flows even in the viscous buffer region.

Recent studies (Jimenez and Hoyas[126] and Buschmann *et al.*[137]) report significant differences for the available $\overline{w^2}^+$ and $\overline{v^2}^+$ profiles between boundary layers and internal flows in the logarithmic region. These measurements are sparse (and difficult to obtain) at high Reynolds numbers, and further work is warranted. Note, however, that all these findings are consistent with the inner region being influenced by outer-scale motions, which have been shown to depend on the outer geometry.

It has become clear that the relative importance of LSMs and VLSMs depends on the nature of the flow: they appear to behave differently in pipes, channels, and boundary layers (Hutchins and Marusic,[114] Bailey *et al.*,[157] and Monty *et al.*[155]). Monty *et al.*[155] concluded that superstructures as reported by Hutchins and Marusic[114] in boundary layers are different from the VSLMs reported by Kim and Adrian[26] in pipe and channel flows. Whether the quantitative differences observed are due to the interaction with the opposite wall in pipe and channel flows or the intermittency of the outer region in boundary layers remains uncertain. Another issue which complicates comparisons is the appropriate Reynolds number for comparison.

E. Roughness

Recent high-Reynolds-number experiments have broadly upheld Townsend's hypothesis that the influence of roughness on the outer region is restricted solely to changing the boundary condition, U_τ. This is found to be so even for large roughness elements, despite their influence extending to about three times their height from the wall. However, anomalous experiments do exist, particularly with two-dimensional roughness in boundary layers, and these will need to be explained.

New roughness experiments have shown that most (but not all) roughness types produce an inflectional (Nikuradse-like) transitional resistance relationship. While Nikuradse's results in rough-wall flows are for the specific sand-grain roughness, they are far more representative of the practical conditions than any of the Colebrook correlations, which are smoothed curves through a variety of practical conditions, but not accurately representative of any of them. This implies that schemes based on Colebrook's interpolation (such as the Moody diagram) have to be phased out gracefully.

F. Experimental methods

The past couple of decades have seen a number of high-Reynolds-number facilities come on line (including all the facilities cited in Table I), with others on the way (CICLoPE and the New Hampshire tunnel). We now recognize that independent measurements of the wall shear stress in all boundary layers (and most channel flows) are essential, with the fully developed pipe flow being the exception. The value of any data is greatly diminished without such independent accompanying measurements. Existing facilities (particularly the channel and pipe flows at Melbourne) have helped to improve our understanding of flow development in fully developed flows.

We also now have a much better appreciation of the effects of initial conditions on boundary layers (from experiments and from DNS). Because boundary layers are generated in flow facilities in many different ways, for instance, on walls of test sections or on suspended plates, with different starting conditions and different devices to achieve the fully turbulent state, the virtual origin of the turbulent boundary layer can vary a great deal. While it is most convenient in practice to correlate the local skin friction with a Reynolds number based on x, such correlations are of very limited use or general validity. The new derivation of streamwise boundary layer growth from the log law and the basic equations has brought about a significant improvement as the virtual origin of ZPG TBLs can now be determined from local integral parameters without the need for additional fitting parameters.

The ASL has proven to be an invaluable and single resource for extremely high-Reynolds-number data, while at the same time we recognize clearly its limitations for providing high quality data and continue to debate its suitability as a model for the canonical case.

We have highlighted the effects of spatial resolution on hot-wire response, which is much more pervasive than previously thought. The development of very small probes to solve this problem for existing facilities is under way and future facilities are generally being designed to overcome the spatial resolution problem by building them on a large enough scale. We have also seen the development of new instrumentation to measure pressure fluctuations within a turbulent flow with good spatial resolution.

G. Modeling and prediction

Nearly all turbulence models, and their computational implementations for the prediction of wall-bounded flows, depend explicitly or implicitly on the overlap region parameters. Therefore, all of the issues raised above have a substantial impact on our ability to *predict* such flows, in particular, for complex flow fields or geometries. For example, the sensitivity of the results to the von Kármán constant alone can lead to unacceptable errors in predictions. Simply relying on calibration of the many coefficients used in these models, which are specific to particular flow geometries over limited ranges of Reynolds number, is not a prudent approach.

VIII. CLOSING REMARKS

Significant work has been carried out over the past decade on wall-bounded turbulence, and this has largely been driven by the desire to generate data at high Reynolds numbers; DNSs have proceeded in a similar way. Even so, many of the outstanding issues listed by Sreenivasan[15] 20 years ago remain open, and, indeed, new experiments have led to new questions related to scaling laws and the role of the largest scale motions. At the moment, extracting a theory by sifting through the data more carefully is the missing element. A positive development is that, perhaps more than ever before, we are starting to develop extensive collaborations, sharing facilities, instrumentation, and ideas. These efforts are likely to be increasingly international and cooperative.

One project, inspired by the workshops and already under way, called ICET (International Collaboration on Experiments in Turbulence) is an attempt to explore the limits of turbulent flow facilities and their instrumentation by a group of scientists drawn from Australia, Italy, Japan, Sweden, Switzerland, and the United States, with experiments carried out jointly in wind tunnels at Stockholm, Melbourne, and Chicago, listed in Table I. Such efforts, and others in the future, are indeed required for a better understanding of high-Reynolds-number turbulence.

ACKNOWLEDGMENTS

We wish to thank all of our colleagues who have contributed to the International Workshop series with their participation and various communications. The International Center for Theoretical Physics, Trieste, and the Ettore Majorano Foundation and Center for Scientific Culture, Erice, are gratefully acknowledged for their financial and managerial support of the 2004 and 2006 workshops, respectively. The financial support of the Australian Research Council (I.M.), the National Science Foundation (B.J.M. and A.J.S.), and the Office of Naval Research (A.J.S.) is also gratefully acknowledged.

[1] F. H. Clauser, "The turbulent boundary layer," Adv. Mech. **4**, 1 (1956).
[2] D. E. Coles and E. A. Hirst, *Proceedings of the Computation of Turbulent Boundary Layers*, AFOSR-IFP-Stanford Conference 1968 (Stanford University, Stanford, 1969), Vol. II.
[3] M. Gad-el-Hak and P. Bandyopadhyay, "Reynolds number effects in wall-bounded turbulent flows," Appl. Mech. Rev. **47**, 307 (1994).
[4] A. A. Townsend, *The Structure of Turbulent Shear Flow* (Cambridge University Press, Cambridge, 1956).
[5] A. A. Townsend, *The Structure of Turbulent Shear Flow*, 2nd ed. (Cambridge University Press, Cambridge, 1976).
[6] D. E. Coles, "The law of the wake in the turbulent boundary layer," J. Fluid Mech. **1**, 191 (1956).
[7] J. C. Rotta, "Turbulent boundary layers in incompressible flow," Prog. Aerosp. Sci. **2**, 1 (1962).
[8] C. M. Millikan, *Proceedings of the Fifth International Congress On Applied Mechanics* (Wiley, New York, 1938).
[9] T. Theodorsen, *Proceedings of the Second Midwestern Conference on Fluid Mechanics, 17–19 March* (Ohio State University, Columbus, OH, 1952).
[10] F. R. Hama, J. D. Long, and J. C. Hegarty, "On transition from laminar to turbulent flow," J. Appl. Phys. **28**, 388 (1957).
[11] S. J. Kline, W. C. Reynolds, F. A. Schraub, and P. W. Rundstadler, "The structure of turbulent boundary layers," J. Fluid Mech. **30**, 741 (1967).
[12] M. R. Head and P. R. Bandyopadhyay, "New aspects of turbulent structure," J. Fluid Mech. **107**, 297 (1981).
[13] A. E. Perry and M. S. Chong, "On the mechanism of wall turbulence," J. Fluid Mech. **119**, 173 (1982).
[14] B. J. Cantwell, "Organised motion in turbulent flow," Annu. Rev. Fluid Mech. **13**, 457 (1981).
[15] K. R. Sreenivasan, in *Frontiers in Experimental Fluid Mechanics*, edited by M. Gad el Hak (Springer-Verlag, New York, 1989).
[16] S. K. Robinson, "Coherent motions in turbulent boundary layers," Annu. Rev. Fluid Mech. **23**, 601 (1991).
[17] R. L. Panton, "Overview of the self-sustaining mechanisms of wall turbulence," Prog. Aerosp. Sci. **37**, 341 (2001).
[18] R. J. Adrian, "Hairpin vortex organization in wall turbulence," Phys. Fluids **19**, 041301 (2007).
[19] P. Bradshaw, "The turbulence structure of equilibrium boundary layers," J. Fluid Mech. **29**, 625 (1967).
[20] I. Marusic and G. J. Kunkel, "Streamwise turbulence intensity formulation for flat-plate boundary layers," Phys. Fluids **15**, 2461 (2003).
[21] M. M. Metzger and J. C. Klewicki, "A comparative study of near-wall turbulence in high and low Reynolds number boundary layers," Phys. Fluids **13**, 692 (2001).
[22] J. F. Morrison, B. J. McKeon, W. Jiang, and A. J. Smits, "Scaling of the streamwise velocity component in turbulent pipe flow," J. Fluid Mech. **508**, 99 (1999).
[23] H. H. Fernholz and P. J. Finley, "The incompressible zero-pressure-gradient turbulent boundary layer: An assessment of the data," Prog. Aerosp. Sci. **32**, 245 (1996).
[24] C. R. Smith and S. P. Metzler, "The characteristics of low-speed streaks in the near-wall region of a turbulent boundary layer," J. Fluid Mech. **129**, 27 (1983).
[25] J. C. Klewicki, M. M. Metzger, E. Kelner, and E. M. Thurlow, "Viscous sublayer flow visualizations at $R_\theta \approx 1500000$," Phys. Fluids **7**, 857 (1995).
[26] K. C. Kim and R. J. Adrian, "Very large-scale motion in the outer layer," Phys. Fluids **11**, 417 (1999).
[27] B. J. McKeon and J. F. Morrison, "Asymptotic scaling in turbulent pipe flow," Philos. Trans. R. Soc. London, Ser. A **365**, 771 (2007).
[28] I. Marusic, "On the role of large-scale structures in wall turbulence," Phys. Fluids **13**, 735 (2001).
[29] B. J. Balakumar and R. J. Adrian, "Large- and very-large scale motions in channel and boundary-layer flows," Proc. R. Soc. London, Ser. A **365**, 665 (2007).
[30] M. V. Zagarola and A. J. Smits, "Mean-flow scaling of turbulent pipe flow," J. Fluid Mech. **373**, 33 (1998).
[31] J. C. Klewicki, J. F. Foss, and J. M. Wallace, in *Flow at Ultra-High Reynolds and Rayleigh Numbers*, edited by R. J. Donnelly and K. R. Sreenivasan (Springer, New York, 1998).
[32] H. M. Nagib, K. A. Chauhan, and P. A. Monkewitz, "Approach to an asymptotic state for zero pressure gradient turbulent boundary layers," Philos. Trans. R. Soc. London, Ser. A **365**, 755 (2007).
[33] J. M. Österlund, A. V. Johansson, H. M. Nagib, and M. H. Hites, "A note on the overlap region in turbulent boundary layers," Phys. Fluids **12**, 1 (2000).
[34] J. Carlier and M. Stanislas, "Experimental study of eddy structures in a turbulent boundary layer using particle image velocimetry," J. Fluid Mech. **535**, 143 (2005).
[35] T. B. Nickels, I. Marusic, S. M. Hafez, and M. S. Chong, "Evidence of the k^{-1} law in a high-Reynolds-number turbulent boundary layer," Phys. Rev. Lett. **95**, 074501 (2005).
[36] D. B. De Graaff and J. K. Eaton, "Reynolds-number scaling of the flat-plate turbulent boundary layer," J. Fluid Mech. **422**, 319 (2000).
[37] R. J. Adrian, C. D. Meinhart, and C. D. Tomkins, "Vortex organization in the outer region of the turbulent boundary layer," J. Fluid Mech. **422**, 1 (2000).
[38] C. D. Tomkins and R. J. Adrian, "Spanwise structure and scale growth in turbulent boundary layers," J. Fluid Mech. **490**, 37 (2003).
[39] C. J. Kähler, "Investigation of the spatio-temporal flow structure in the buffer region of a turbulent boundary layer by means of multiple plane stereo PIV," Exp. Fluids **36**, 114 (2004).
[40] B. Ganapathisubramani, E. K. Longmire, and I. Marusic, "Characteristics of vortex packets in turbulent boundary layers," J. Fluid Mech. **478**, 35 (2003).
[41] W. T. Hambleton, N. Hutchins, and I. Marusic, "Simultaneous orthogonal-plane particle image velocimetry measurements in a turbulent boundary layer," J. Fluid Mech. **560**, 53 (2006).
[42] G. E. Elsinga, R. J. Adrian, B. W. van Oudheusden, and F. Scarano, *Seventh International Symposium on Particle Image Velocimetry*, Rome, Italy, 2007 (Sapienza University of Rome, Rome, 2007).
[43] R. D. Moser, J. Kim, and N. N. Mansour, "Direct numerical simulation of turbulent channel flow up to $R_\tau=590$," Phys. Fluids **11**, 943 (1999).
[44] H. Abe, H. Kawamura, and H. Choi, "Very large-scale structures and their effects on the wall shear-stress fluctuations in a turbulent channel flow up to $\mathrm{Re}_\tau=640$," J. Fluids Eng. **126**, 835 (2004).
[45] K. Iwamoto, T. Tsukahara, H. Nakano, and H. Kawamura, in *IUTAM Symposium on Computational Physics and New Perspectives in Turbulence*, edited by Y. Kaneda (Springer, New York, 2006), pp. 53–58.
[46] J. C. del Álamo, J. Jiménez, P. Zandonade, and R. D. Moser, "Self-similar vortex clusters in the turbulent logarithmic region," J. Fluid Mech. **561**, 329 (2006).
[47] S. Hoyas and J. Jiménez, "Scaling of the velocity fluctuations in turbulent channels up to $\mathrm{Re}_\tau=2003$," Phys. Fluids **18**, 011702 (2006).

[48]Z. Hu, C. Morley, and N. Sandman, "Wall pressure and shear stress spectra from direct simulations of channel flow," AIAA J. **44**, 1541 (2006).
[49]P. A. Monkewitz, K. A. Chauhan, and H. M. Nagib, "Self-contained high-Reynolds-number asymptotics for zero-pressure-gradient turbulent boundary layers," Phys. Fluids **19**, 115101 (2007).
[50]G. I. Barenblatt, A. J. Chorin, O. H. Hald, and V. M. Prostokishin, "Structure of the zero-pressure-gradient turbulent boundary layer," Proc. Natl. Acad. Sci. U.S.A. **94**, 7817 (1997).
[51]W. K. George and L. Castillo, "Zero-pressure-gradient turbulent boundary layer," Appl. Mech. Rev. **50**, 689 (1997).
[52]J. C. Klewicki, P. Fife, T. Wei, and P. McMurtry, "A physical model of the turbulent boundary layer consonant with mean momentum balance structure," Philos. Trans. R. Soc. London, Ser. A **365**, 823 (2007).
[53]B. J. McKeon and K. R. Sreenivasan, "Introduction: Scaling and structure in high Reynolds number wall-bounded flows," Philos. Trans. R. Soc. London, Ser. A **365**, 635 (2007).
[54]B. J. McKeon, J. Li, W. Jiang, J. F. Morrison, and A. J. Smits, "Further observations on the mean velocity distribution in fully developed pipe flow," J. Fluid Mech. **501**, 135 (1999).
[55]J. P. Monty, "Developments in smooth wall turbulent duct flows," Ph.D. thesis, University of Melbourne, 2005.
[56]E.-S. Zanoun, F. Durst, and H. Nagib, "Evaluating the law of the wall in two-dimensional fully developed turbulent channel flows," Phys. Fluids **10**, 1 (2003).
[57]T. B. Nickels, I. Marusic, S. M. Hafez, N. Hutchins, and M. S. Chong, "Some predictions of the attached eddy model for a high Reynolds number boundary layer," Philos. Trans. R. Soc. London, Ser. A **365**, 807 (2007).
[58]R. Duncan, N. Hutchins, J. Monty, and A. Segalini, *APS/DFD Meeting*, 2009 (University of Minnesota, Minneapolis, 2009).
[59]A. Talamelli, F. Persiani, J. H. M. Fransson, H. Alfredsson, A. V. Johansson, H. M. Nagib, J. D. Ruedi, K. R. Sreenivasan, and P. A. Monkewitz, "CICLoPE—A response to the need for high Reynolds number experiments," Fluid Dyn. Res. **41**, 021407 (2009).
[60]J. C. Klewicki, private communication.
[61]M. Metzger, "Scalar dispersion in high Reynolds number turbulent boundary layers," Ph.D. thesis, University of Utah, 2002.
[62]I. Marusic and N. Hutchins, "Study of the log-layer structure in wall turbulence over a very large range of Reynolds number," Flow, Turbul. Combust. **81**, 115 (2008).
[63]J. C. Klewicki, P. J. A. Priyadarshana, and M. M. Metzger, "Statistical structure of the fluctuating wall pressure and its in-plane gradients at high Reynolds number," J. Fluid Mech. **609**, 195 (2008).
[64]J. D. Ruedi, H. M. Nagib, J. Osterlund, and P. A. Monkewitz, "Evaluation of three techniques for wall-shear measurements in three-dimensional flows," Exp. Fluids **35**, 389 (2003).
[65]H. H. Fernholz, G. Janke, M. Schober, P. M. Wagner, and D. Warnack, "New developments and applications of skin-friction measuring techniques," Meas. Sci. Technol. **7**, 1396 (1996).
[66]J. Nikuradse, "Gesetzimassen der turbuleuten Stromung in glatten Rohren," VDI-Forschungsh. **356**, 289 (1932).
[67]A. E. Perry, S. M. Henbest, and M. S. Chong, "A theoretical and experimental study of wall turbulence," J. Fluid Mech. **165**, 163 (1986).
[68]J. Doherty, P. Ngan, J. P. Monty, and M. S. Chong, in *Proceedings of the 16th Australasian Fluid Mechanics Conference*, edited by P. A. Jacobs, T. J. McIntyre, M. J. Cleary, D. Buttsworth, D. J. Mee, R. Clements, R. G. Morgan, and C. Lemckert, University of Queensland, 2007 (The University of Queensland, Brisbane, 2007), pp. 266–270.
[69]K. Lien, J. P. Monty, M. S. Chong, and A. Ooi, *Proceedings of the 15th Australasian Fluid Mechanics Conference*, 2004 (The University of Sydney, Sydney, 2004).
[70]E.-S. Zanoun, H. M. Nagib, and F. Durst, "Refined C_f relation for turbulent channels and consequences for high Re experiments," Fluid Dyn. Res. **41**, 021405 (2009).
[71]X. Wu and P. Moin, "A direct numerical simulation study on the mean velocity characteristics in turbulent pipe flow," J. Fluid Mech. **608**, 81 (2008).
[72]R. Narasimha and A. Prabhu, "Equlibrium and relaxation in turbulent wakes," J. Fluid Mech. **54**, 1 (1972).
[73]M. B. Jones, I. Marusic, and A. E. Perry, "Evolution and structure of sink flow turbulent boundary layers," J. Fluid Mech. **428**, 1 (2001).
[74]D. E. Coles, "The turbulent boundary layer in a compressible field," USAF The Rand Cooperation Technical Report No. R-403-PR, 1962.
[75]L. Castillo and T. G. Johansson, "The effects of the upstream conditions on a low Reynolds number turbulent boundary layer with zero pressure gradient," J. Turbul. **3**, 031 (2002).
[76]P. A. Monkewitz, K. A. Chauhan, and H. M. Nagib, "Comparison of mean flow similarity laws in zero pressure gradient turbulent boundary layers," Phys. Fluids **20**, 105102 (2008).
[77]K. A. Chauhan and H. M. Nagib, in *IUTAM Symposium on Computational Physics and New Perspectives in Turbulence*, edited by Y. Kaneda (Springer, New York, 2006), pp. 177–182.
[78]L. Castillo and D. J. Walker, "Effect of upstream conditions on the outer flow of turbulent boundary layers," AIAA J. **40**, 1292 (2002).
[79]K. A. Chauhan, P. A. Monkewitz, and H. M. Nagib, "Criteria for assessing experiments in zero pressure gradient boundary layers," Fluid Dyn. Res. **41**, 021404 (2009).
[80]A. E. Perry, I. Marusic, and J. D. Li, "Wall turbulence closure based on classical similarity laws and the attached eddy hypothesis," Phys. Fluids **6**, 1024 (1994).
[81]A. E. Perry, I. Marusic, and M. B. Jones, "On the streamwise evolution of turbulent boundary layers in arbitrary pressure gradients," J. Fluid Mech. **461**, 61 (2002).
[82]A. E. Perry, I. Marusic, and M. B. Jones, "New evolution equations for turbulent boundary layers in arbitrary pressure gradients," Sadhana: Proc., Indian Acad. Sci. **23**, 443 (1998).
[83]T. Wei, P. Fife, J. C. Klewicki, and P. McMurtry, "Properties of the mean momentum balance in turbulent boundary layer, pipe and channel flows," J. Fluid Mech. **522**, 303 (1999).
[84]R. R. Long and T. C. Chen, "Experimental evidence for the existence of the 'mesolayer' in turbulent systems," J. Fluid Mech. **105**, 19 (1981).
[85]N. Afzal, "Fully turbulent flow in a pipe-an intermediate layer," Ing.-Arch. **52**, 355 (1982).
[86]K. R. Sreenivasan, in *Turbulence Management and Relaminarization*, edited by H. W. Liepmann and R. Narasimha (Springer-Verlag, New York, 1987).
[87]J. Kevorkian and J. D. Cole, *Perturbation Methods in Applied Mathematics* (Springer, New York, 1985).
[88]M. Wosnik, L. Castillo, and W. K. George, "A theory for turbulent pipe and channel flows," J. Fluid Mech. **421**, 115 (2000).
[89]M. Oberlack, "A unified approach for symmetries in plane parallel turbulent shear flows," J. Fluid Mech. **427**, 299 (2001).
[90]B. Lindgren, J. M. Osterlund, and A. V. Johansson, "Evaluation of scaling laws derived from Lie group symmetry methods in zero-pressure-gradient turbulent boundary layers," J. Fluid Mech. **502**, 127 (1999).
[91]P. R. Spalart, G. R. Coleman, and R. Johnstone, "Direct numerical simulation of the Ekman layer: A step in Reynolds number, and cautious support for a log law with a shifted origin," Phys. Fluids **20**, 101507 (2008).
[92]G. I. Barenblatt, "Scaling laws for fully developed turbulent shear flows. Part 1. Basic hypotheses and analysis," J. Fluid Mech. **248**, 513 (1993).
[93]W. K. George, "Recent advancements toward the understanding of turbulent boundary layers," AIAA J. **44**, 2435 (2006).
[94]W. K. George, "Is there a universal log law for turbulent wall-bounded flows?" Philos. Trans. R. Soc. London, Ser. A **365**, 789 (2007).
[95]M. B. Jones, T. B. Nickels, and I. Marusic, "On the asymptotic similarity of the zero pressure-gradient turbulent boundary layer," J. Fluid Mech. **616**, 195 (2008).
[96]R. L. Panton, "Composite asymptotic expansions and scaling wall turbulence," Philos. Trans. R. Soc. London, Ser. A **365**, 733 (2007).
[97]B. J. McKeon, "High Reynolds number turbulent pipe flow," Ph.D. thesis, Princeton University, 2003.
[98]J. Jiménez and R. D. Moser, "What are we learning from simulating wall turbulence?" Philos. Trans. R. Soc. London, Ser. A **365**, 715 (2007).
[99]N. Afzal, "Millikan's argument at moderately large Reynolds number," Phys. Fluids **19**, 600 (1976).
[100]K. R. Sreenivasan and A. Sahay, in *Self-Sustaining Mechanisms of Wall Turbulence*, edited by R. Panton (WIT Press, Southampton, 1997), pp. 253–272.
[101]P. A. Monkewitz and H. M. Nagib, "The Reynolds shear stress in zero pressure gradient turbulent boundary layers derived from log-law asymptotics," Bull. Am. Phys. Soc. **53**, 97 (2008).
[102]K. A. Chauhan, H. M. Nagib, and P. A. Monkewitz, in *Progress in Turbulence 2. Proceedings of iTi Conference in Turbulence*, edited by M. Oberlack, G. Khujadze, S. Guenther, T. Weller, M. Frewer, J. Peinke, and S. Barth (Springer, New York, 2007), pp. 159–163.
[103]H. M. Nagib and K. A. Chauhan, "Variations of von Kármán coefficient in canonical flows," Phys. Fluids **20**, 101518 (2008).

[104] R. L. Panton, "Review of wall turbulence as described by composite expansions," Appl. Mech. Rev. **58**, 1 (2005).
[105] P. R. Spalart, "Direct simulation of turbulent boundary layer up to $R_\theta=1410$," J. Fluid Mech. **187**, 61 (1988).
[106] H. M. Nagib, C. Christophorou, and P. A. Monkewitz, "High Reynolds number turbulent boundary layers subjected to various pressure-gradient conditions," in *IUTAM Symposium on One Hundred Years of Boundary Layer Research*, DLR Göttingen, Germany, 12–14 August 2004, edited by G. E. A. Meier and K. R. Sreenivasan (Springer, Berlin, 2004), pp. 383–394.
[107] S. A. Dixit and O. N. Ramesh, "Pressure-gradient-dependent logarithmic laws in sink flow turbulent boundary layers," J. Fluid Mech. **615**, 445 (2008).
[108] C. Bourassa and F. O. Thomas, "An experimental investigation of a highly accelerated turbulent boundary layer," J. Fluid Mech. **634**, 359 (2009).
[109] F. A. MacMillan, "Experiments on Pitot-tubes in shear flow," Ministry of Supply, Aeronautical Research Council Technical Report No. R&M 3028, 1956.
[110] B. J. McKeon, J. D. Li, W. Jiang, J. F. Morrison, and A. J. Smits, "Pitot probe corrections in fully-developed turbulent pipe flow," Meas. Sci. Technol. **14**, 1449 (2003).
[111] B. J. McKeon and A. J. Smits, "Static pressure correction in high Reynolds number fully developed turbulent pipe flow," Meas. Sci. Technol. **13**, 1608 (2002).
[112] A. E. Perry and I. Marusic, "A wall-wake model for the turbulence structure of boundary layers. Part 1. Extension of the attached eddy hypothesis," J. Fluid Mech. **298**, 361 (1995).
[113] N. Hutchins and I. Marusic, "Large-scale influences in near-wall turbulence," Philos. Trans. R. Soc. London, Ser. A **365**, 647 (2007).
[114] N. Hutchins and I. Marusic, "Evidence of very long meandering streamwise structures in the logarithmic region of turbulent boundary layers," J. Fluid Mech. **579**, 1 (2007).
[115] N. Hutchins, T. B. Nickels, I. Marusic, and M. S. Chong, "Hot-wire spatial resolution issues in wall-bounded turbulence," J. Fluid Mech. **635**, 103 (2009).
[116] J. C. Wyngaard, "Measurements of small scale turbulence structure with hot-wires," J. Sci. Instrum. **1**, 1105 (1968).
[117] S. Mochizuki and F. T. M. Nieuwstadt, "Reynolds-number-dependence of the maximum in the streamwise velocity fluctuations in wall turbulence," Exp. Fluids **21**, 218 (1996).
[118] J. C. Klewicki and R. E. Falco, "On accurately measuring statistics associated with small-scale structure in turbulent boundary layers using hot-wire probes," J. Fluid Mech. **219**, 119 (1990).
[119] M. M. Metzger, J. C. Klewicki, K. L. Bradshaw, and R. Sadr, "Scaling the near-wall axial turbulent stress in the zero pressure gradient boundary layer," Phys. Fluids **13**, 1819 (2001).
[120] H. H. Fernholz, E. Krause, M. Nockemann, and M. Schober, "Comparative measurements in the canonical boundary layer at $\mathrm{Re}_\theta \le 6\times10^4$ on the wall of the DNW," Phys. Fluids **7**, 1275 (1995).
[121] I. Marušic and A. E. Perry, "A wall wake model for the turbulent structure of boundary layers. Part 2. Further experimental support," J. Fluid Mech. **298**, 389 (1995).
[122] J. C. R. Hunt, N. D. Sandham, J. C. Vassilicos, B. E. Launder, P. A. Monkewitz, and G. F. Hewitt, "Developments in turbulence research: A review based on the 1999 programme of the Isaac Newton Institute, Cambridge," J. Fluid Mech. **436**, 353 (2001).
[123] J. F. Morrison, "The interaction between inner and outer regions of turbulent wall-bounded flow," Philos. Trans. R. Soc. London, Ser. A **365**, 683 (2007).
[124] P. A. Davidson, T. B. Nickels, and P. A. Krogstad, "The logarithmic structure function law in wall-layer turbulence," J. Fluid Mech. **550**, 51 (2006).
[125] J. C. R. Hunt and J. F. Morrison, "Eddy structure in turbulent boundary layers," Eur. J. Mech. B/Fluids **19**, 673 (2000).
[126] J. Jiménez and S. Hoyas, "Turbulent fluctuations above the buffer layer of wall-bounded flows," J. Fluid Mech. **611**, 215 (2008).
[127] J. P. Monty and M. S. Chong, "Turbulent channel flow: comparison of streamwise velocity data from experiments and direct numerical simulation," J. Fluid Mech. **633**, 461 (2009).
[128] P. E. Dimotakis, "The mixing transition in turbulent flows," J. Fluid Mech. **409**, 69 (2000).
[129] N. Marati, C. M. Casciola, and R. Piva, "Energy cascade and spatial fluxes in wall turbulence," J. Fluid Mech. **521**, 191 (1999).
[130] G. J. Kunkel, C. B. Arnold, and A. J. Smits, *Proceedings of the 36th AIAA Fluid Dynamics Conference*, 2006 (American Institute of Aeronautics and Astronautics, San Francisco, 2006).
[131] A. E. Perry and J. D. Li, "Experimental support for the attached eddy hypothesis in zero-pressure-gradient turbulent boundary layers," J. Fluid Mech. **218**, 405 (1990).
[132] Y. Tsuji, J. H. M. Fransson, P. H. Alfredsson, and A. V. Johansson, "Pressure statistics and their scaling in high-Reynolds-number turbulent boundary layers," J. Fluid Mech. **585**, 1 (2007).
[133] G. J. Kunkel and I. Marusic, "Study of the near-wall-turbulent region of the high-Reynolds-number boundary layer using an atmospheric flow," J. Fluid Mech. **548**, 375 (2006).
[134] R. Zhao and A. J. Smits, "Scaling of the wall-normal turbulence component in high-Reynolds-number pipe flow," J. Fluid Mech. **576**, 457 (2007).
[135] P. A. Durbin and B. A. Pettersson-Reif, *Statistical Theory and Modeling for Turbulent Flows* (Wiley, New York, 2001).
[136] M. J. Lighthill, in *Laminar Boundary Layers*, edited by L. Rosenhead (Clarendon, Oxford, 1963).
[137] M. H. Buschmann, T. Kempe, T. Indinger, and M. Gad-el-Hak, in *Turbulence, Heat and Mass Transfer*, edited by Y. Nagano, K. Hanjalic, and S. Jakirlic (Begell House, New York, 2009), Vol. 6.
[138] W. Schoppa and F. Hussain, "Coherent structure generation in near-wall turbulence," J. Fluid Mech. **453**, 57 (2002).
[139] P. Chakraborty, S. Balachandar, and R. J. Adrian, "On the relationships between local vortex identification schemes," J. Fluid Mech. **535**, 189 (2005).
[140] X. Wu and P. Moin, "Direct numerical simulation of turbulence in a nominally-zero-pressure-gradient flat-plate boundary layer," J. Fluid Mech. **630**, 5 (2009).
[141] I. Marusic, "Unravelling near walls turbulence," J. Fluid Mech. **630**, 1 (2009).
[142] P. Schlatter, R. Orlu, Q. Li, G. Brethouwer, J. H. M. Fransson, A. V. Johansson, P. H. Alfredsson, and D. S. Henningson, "Turbulent boundary layers up to $\mathrm{Re}_\theta=2500$ studied through simulation and experiment," Phys. Fluids **21**, 051702 (2009).
[143] A. Ferrante and S. Elghobashi, "On the physical mechanisms of drag reduction in a spatially developing turbulent boundary layer laden with microbubbles," J. Fluid Mech. **503**, 345 (1999).
[144] A. Ferrante and S. Elghobashi, "Reynolds number effect on drag reduction in a microbubble-laden spatially developing turbulent boundary layer," J. Fluid Mech. **543**, 93 (2005).
[145] M. Stanislas, L. Perret, and J.-M. Foucaut, "Vortical structures in the turbulent boundary layer: A possible route to a universal representation," J. Fluid Mech. **602**, 327 (2008).
[146] J. Zhou, R. J. Adrian, S. Balachandar, and T. M. Kendall, "Mechanisms for generating coherent packets of hairpin vortices in channel flow," J. Fluid Mech. **387**, 353 (1999).
[147] K. Kim, H. J. Sung, and R. J. Adrian, "Effects of background noise on generating coherent packets of hairpin vortices," Phys. Fluids **20**, 105107 (2008).
[148] R. E. Falco, "Coherent motions in the outer region of turbulent boundary layers," Phys. Fluids **20**, S124 (1977).
[149] C. R. Smith, J. D. A. Walker, A. H. Haidari, and U. Soburn, "On the dynamics of near-wall turbulence," Philos. Trans. R. Soc. London, Ser. A **336**, 131 (1991).
[150] Y. Wu and K. T. Christensen, "Population trends of spanwise vortices in wall turbulence," J. Fluid Mech. **568**, 55 (2006).
[151] V. K. Natrajan, Y. Wu, and K. T. Christensen, "Spatial signatures of retrograde spanwise vortices in wall turbulence," J. Fluid Mech. **574**, 155 (2007).
[152] B. Ganapathisubramani, N. Hutchins, W. T. Hambleton, E. K. Longmire, and I. Marusic, "Investigation of large-scale coherence in a turbulent boundary layer using two-point correlations," J. Fluid Mech. **524**, 57 (1999).
[153] N. Hutchins, B. Ganapathisubramani, and I. Marusic, "Inclined cross-stream stereo particale image velocimetry measurements in turbulent boundary layers," J. Fluid Mech. **541**, 21 (2005).
[154] S. C. Morris, S. R. Stolpa, P. E. Slaboch, and J. C. Klewicki, "Near surface particle image velocimetry measurements in a transitionally rough-wall atmospheric surface layer," J. Fluid Mech. **580**, 319 (2007).
[155] J. P. Monty, N. Hutchins, H. C. H. Ng, I. Marusic, and M. S. Chong, "A comparison of turbulent pipe, channel and boundary layer flows," J. Fluid Mech. **632**, 431 (2009).

[156] J. P. Monty, J. A. Stewart, R. C. Williams, and M. S. Chong, "Large-scale features in turbulent pipe and channel flows," J. Fluid Mech. **589**, 147 (2007).
[157] S. C. C. Bailey, M. N. Hultmark, A. J. Smits, and M. P. Schultz, "Two-point velocity measurements in turbulent pipe flow," J. Fluid Mech. **615**, 121 (2008).
[158] J. Jiménez, J. C. del Álamo, and O. Flores, "The large-scale dynamics of near-wall turbulence," J. Fluid Mech. **505**, 179 (1999).
[159] R. J. Volino, M. P. Schultz, and K. A. Flack, "Turbulence structure in rough- and smooth-wall boundary layers," J. Fluid Mech. **592**, 263 (2007).
[160] D. J. C. Dennis and T. B. Nickels, "On the limitations of taylor's hypothesis in constructing long structures in a turbulent boundary layer," J. Fluid Mech. **614**, 197 (2008).
[161] M. Metzger, B. J. McKeon, and H. Holmes, "The near-neutral atmospheric surface layer: Turbulence and non-stationarity," Philos. Trans. R. Soc. London, Ser. A **365**, 859 (2007).
[162] M. H. Hites, "Scaling of high-Reynolds number turbulent boundary layers in the National Diagnostic Facility," Ph.D. thesis, Illinois Institute of Technology, 1997.
[163] J. C. del Álamo and J. Jiménez, "Spectra of the very large anisotropic scales in turbulent channels," Phys. Fluids **15**, L41 (2003).
[164] K. N. Rao, R. Narasimha, and M. A. Badri Narayanan, "The 'bursting' phenomena in a turbulent boundary layer," J. Fluid Mech. **48**, 339 (1971).
[165] C. E. Wark and H. M. Nagib, "Experimental investigation of coherent structures in turbulent boundary layers," J. Fluid Mech. **230**, 183 (1991).
[166] S. Toh and T. Itano, "Interaction between a large-scale structure and near-wall structures in channel flow," J. Fluid Mech. **524**, 249 (1999).
[167] S. F. Tardu, "Stochastic synchronization of the near wall turbulence," Phys. Fluids **20**, 045105 (2008).
[168] R. Mathis, N. Hutchins, and I. Marusic, "Large-scale amplitude modulation of the small-scale structures in turbulent boundary layers," J. Fluid Mech. **628**, 311 (2009).
[169] I. Marusic and W. D. C. Heuer, "Reynolds number invariance of the structure inclination angle in wall turbulence," Phys. Rev. Lett. **99**, 114504 (2007).
[170] J. C. del Álamo and J. Jiménez, "Linear energy amplification in turbulent channels," J. Fluid Mech. **559**, 205 (2006).
[171] G. Pujals, M. Garcia-Villalba, C. Cossu, and S. Depardon, "A note on optimal transient growth in turbulent channel flows," Phys. Fluids **21**, 015109 (2009).
[172] C. Cossu, G. Pujals, and S. Depardon, "Optimal transient growth and very large–scale structures in turbulent boundary layers," J. Fluid Mech. **619**, 79 (2009).
[173] M. Guala, S. E. Hommema, and R. J. Adrian, "Large-scale and very-large-scale motions in turbulent pipe flow," J. Fluid Mech. **554**, 521 (2006).
[174] J. Jiménez, "Turbulent flows over rough walls," Annu. Rev. Fluid Mech. **36**, 173 (2004).
[175] J. J. Allen, M. A. Shockling, G. J. Kunkel, and A. J. Smits, "Turbulent flow in smooth and rough pipes," Philos. Trans. R. Soc. London, Ser. A **365**, 699 (2007).
[176] K. A. Flack, M. P. Schultz, and T. A. Shapiro, "Experimental support for Townsend's Reynolds number similarity hypothesis on rough walls," Phys. Fluids **17**, 035102 (2005).
[177] P.-A. Krogstad and R. A. Antonia, "Structure of turbulent boundary layers on smooth and rough walls," J. Fluid Mech. **277**, 1 (1994).
[178] P.-A. Krogstadt and R. A. Antonia, "Surface roughness effects in turbulent boundary layers," Exp. Fluids **27**, 450 (1999).
[179] M. A. Shockling, J. J. Allen, and A. J. Smits, "Roughness effects in turbulent pipe flow," J. Fluid Mech. **564**, 267 (2006).
[180] S. E. Hommema and R. J. Adrian, "Packet structure of surface eddies in the atmospheric boundary layer," Boundary-Layer Meteorol. **106**, 147 (2003).
[181] A. E. Perry, S. Hafez, and M. S. Chong, "A possible reinterpretation of the Princeton superpipe data," J. Fluid Mech. **439**, 395 (2001).
[182] M. P. Schultz and K. A. Flack, "The rough-wall turbulent boundary layer from the hydraulically smooth to the fully rough regime," J. Fluid Mech. **580**, 381 (2007).
[183] L. I. Langelandsvik, G. J. Kunkel, and A. J. Smits, "Flow in a commercial steel pipe," J. Fluid Mech. **595**, 323 (2007).
[184] C. F. Colebrook, "Turbulent flow in pipes, with particular reference to the transitional region between smooth and rough wall laws," J. Inst. Chem. Eng. **11**, 133 (1939).
[185] J. J. Allen, M. A. Shockling, and A. J. Smits, "Evaluation of a universal transitional resistance diagram for pipes with honed surfaces," Phys. Fluids **17**, 121702 (2005).
[186] G. Gioia and P. Chakraborty, "Turbulent friction in rough pipes and the energy spectrum of the phenomenological theory," Phys. Rev. Lett. **96**, 044502 (2006).
[187] S. H. Lee and H. J. Sung, "Direct numerical simulation of the turbulent boundary layer over a rod-roughened wall," J. Fluid Mech. **584**, 125 (2007).
[188] P.-Å. Krogstad, H. I. Andersson, O. M. Bakken, and A. Ashrafian, "An experimental and numerical study of channel flow with rough walls," J. Fluid Mech. **530**, 327 (1999).
[189] D. G. Crighton and F. G. Leppington, "Singular perturbation methods in acoustics—diffraction by a plate of finite thickness," Philos. Trans. R. Soc. London, Ser. A **335**, 313 (1973).
[190] L. S. G. Kovasznay, V. Kibens, and R. F. Blackwelder, "Large-scale motion in the intermittent region of a turbulent boundary layer," J. Fluid Mech. **41**, 283 (1970).